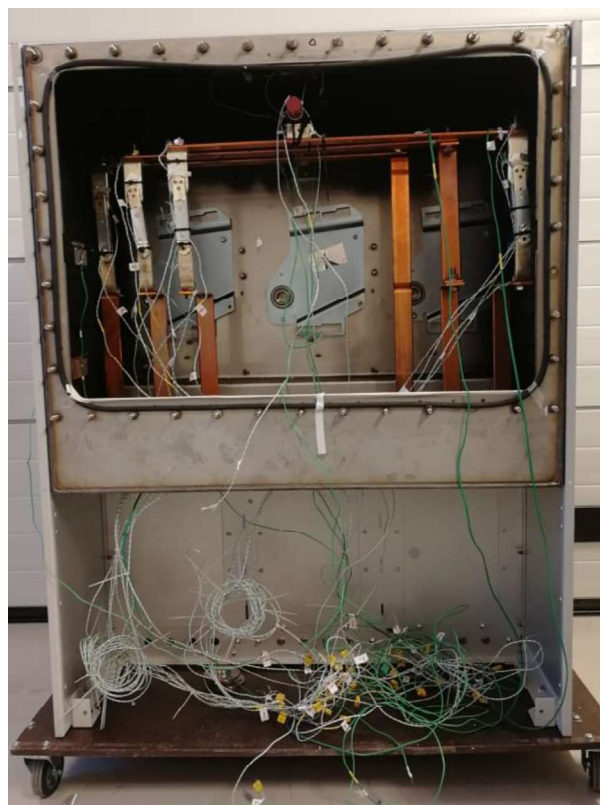


FMH606 Master's Thesis 2019
Electrical Power Engineering

Influence of thermal radiation in MV switchgear



Tonje Gløsmyr

Course: FMH606 Master's Thesis, 2019

Title: Influence of thermal radiation in MV switchgear

Number of pages: 82

Keywords: MV switchgear, temperature rise tests, thermal radiation, emissivity

Student: Tonje Gløsmyr
Supervisor: Elin Fjeld, Wilhelm Rondeel
External partner: ABB AS
Availability: Open

Summary:

When developing MV switchgear units it is important that the finalized product is within IEC maximum temperature rise limit. When a switchgear unit is developed it is continuously tested until it meets the requirements, the process may be time consuming, costly and involve several prototypes. A method who can decrease the number of tests and minimize the cost and time, is to use simulation tools to simulate the temperature rise. One challenges when simulation temperature rise is to find the thermal radiation, as it is difficult to estimate.

The purpose of this report is to estimate how much of the power loss goes to thermal radiation in a MV switchgear unit with 630 A, 500 A, 400 A and 200 A current load, with both painted and non-painted current conductors. This will be done experimentally by measuring the temperature, the emissivity and the resistance and use this to estimate the power loss and the thermal radiation.

For unpainted conductors the silver coated switch contributes with 10 % thermal radiation of the power loss in the switch. The temperature rise is higher with unpainted conductors and the thermal radiation is lower. For unpainted conductors the switch contributed with 45-50 % of the power loss in the switch. Painting, coating or using other methods to rise the emissivity lowers the temperature rise and increases the contribution of thermal radiation. It is crucial to take the thermal radiation into account for objects with higher emissivity, as the contributes with more thermal radiation.

The University of South-Eastern Norway takes no responsibility for the results and conclusions in this student report.

Preface

This master thesis is written in spring 2019 and is a part of the master's degree "Electrical power engineering". The report is aimed at people with general knowledge within electric power, with interest in heat transfer mechanisms.


Data tools used in the report are MS Word, MS Excel, MS Visio, MS Project, Agilent BenchLink Data Logger 3, SmartView® and SolidWorks.

Cover image is photographed by Tonje Gløsmyr.

I would like to thank all who have helped and contributed to the report, especially:

Elin Fjeld

Porsgrunn, 14.05.2019


Tonje Gløsmyr

Contents

Preface	3
Contents.....	4
Nomenclature	6
1 Introduction	9
1.1 Background	9
1.2 Objective.....	9
1.3 Report structure.....	10
2 Theory	11
2.1 MV switchgear unit and RMU	11
2.2 Power loss MV switchgear.....	12
2.2.1 Resistance	12
2.3 Dynamic and stationary temperature rise	14
2.3.1 Maximum temperature rise in switchgear	15
2.4 The Heat transfer mechanisms	16
2.4.1 Conduction	16
2.4.2 Convection.....	17
2.4.3 Radiation	17
3 System and equipment.....	20
3.1 The test device	20
3.1.1 Paint.....	22
3.2 The equipment	23
3.2.1 The current injector	23
4 Surface area estimation.....	25
4.1 Equipment	25
4.2 Procedure	25
4.3 Result	26
5 Emissivity measurements	27
5.1 Equipment	27
5.2 Procedure	27
5.2.1 Method 1: Thermocouple elements.....	28
5.2.2 Method 2: Tape	28
5.3 Result	30
6 Resistance measurement and power loss estimation	31
6.1 Equipment	31
6.2 Procedure	31
6.2.1 Cold resistance	31
6.2.2 Warm resistance	32
6.3 Result	32
6.3.1 The cold resistance of the components	32
6.3.2 The warm resistance for the phases.....	33
6.3.3 The warm resistance in the copper bars	35
6.3.4 The warm resistance in the switches.....	36

6.4 Estimated power loss	39
6.4.1 <i>The power loss for each component in phase L1</i>	40
7 Temperature rise test.....	41
7.1 Equipment	41
7.2 Procedure	41
7.3 Result	42
7.3.1 <i>Unpainted</i>	42
7.3.2 <i>Painted</i>	43
7.3.3 <i>The temperature rise in L1</i>	44
8 Thermal radiation estimation	46
8.1 Procedure	46
8.2 Result	47
8.2.1 <i>Thermal radiation with unpainted conductors</i>	47
8.2.2 <i>Thermal radiation with painted conductors</i>	48
9 Discussion	51
9.1 Influence of thermal radiation	51
9.2 Parameters who influences the thermal radiation estimate.....	51
9.2.1 <i>The MV switchgear test devise</i>	51
9.2.2 <i>The view factor</i>	52
9.2.3 <i>The emissivity</i>	52
9.2.4 <i>The surface area</i>	52
9.2.5 <i>The temperature rise test</i>	53
9.2.6 <i>Total power loss</i>	53
10 Conclusion.....	54
Referanser	55
Appendices.....	57

Nomenclature

AC	Alternating current
Ag	Silver
Cigré	International Council on Large Electrical Systems
Cold resistance	The resistance at initial temperature
Cu	Copper
DC	Direct current
IEC	International electrotechnical commission
LBS	Load breaker switch
MV	Medium voltage (1 kV to 33 kV)
RMU	Ring main unit
Steady state temperature	Temperature rise $>1\text{ }^{\circ}\text{C/h}$
USN	University of Southeast Norway
Warm resistance	The resistance at steady state temperature

Symbols

P	<i>Power loss</i>	[W]
R	<i>Resistance</i>	[Ω]
I	<i>Current</i>	[A]
ρ	<i>The specific resistance</i>	[Ωm]
A	<i>Surface area</i>	[m^2]
l	<i>Length</i>	[m]
V	<i>Volume</i>	[m^3]
σ	<i>Cross section</i>	[m^2]
T_s	<i>Surface temperature</i>	[$^{\circ}\text{K}$] or [$^{\circ}\text{C}$]
T_a	<i>Air temperature</i>	[$^{\circ}\text{K}$] or [$^{\circ}\text{C}$]
T_0	<i>Initial temperature</i>	[$^{\circ}\text{K}$] or [$^{\circ}\text{C}$]
T_w	<i>Wall temperature</i>	[$^{\circ}\text{K}$] or [$^{\circ}\text{C}$]
ΔT	<i>Temperature change</i>	[$^{\circ}\text{K}$] or [$^{\circ}\text{C}$]
Δ	<i>Delta</i>	[change]
α	<i>Temperature coefficient</i>	$\left[\frac{1}{^{\circ}\text{C}}\right]$
c	<i>Specific heat</i>	$\left[\frac{\text{J}}{\text{kg} * ^{\circ}\text{K}}\right]$
γ	<i>Density</i>	$\left[\frac{\text{kg}}{\text{m}^3}\right]$
h	<i>Heat transfer coefficient</i>	$\left[\frac{\text{W}}{\text{m}^2} * ^{\circ}\text{K}\right]$
λ	<i>Thermal conductivity</i>	$\left[\frac{\text{W}}{\text{m}} ^{\circ}\text{C}\right]$

σ_s *Stefan Boltzmann constant*

f *View factor*

ε *Emissivity*

1 Introduction

This chapter explains the background, objective and the report structure.

1.1 Background

When developing MV switchgear unit, it is important to know the maximum temperature rise and the steady state temperature the switchgear will have during operation. High temperatures may increase the degradation mechanisms and lower the lifespan of the switchgear. IEC has therefor set temperature limits which the switchgear should not exceeds but be as close to as possible to utilize the efficiency of the switchgear as much as possible.

In the process of developing the switchgear it is therefore important to continuously test the switchgear design and performance until the temperature matches the requirements. Testing the design continuously in developing process may be expensive and time-consuming. One method who is increasingly more common to use to minimize the cost and time is to use simulation tools. This is used to simulate the temperature rise with the switchgear design. This allows the user to make changes in a 3D model without having to build a new switchgear unit and redo the temperature test for every little tweak.

One of the challenges with using simulation tools to simulate the temperature rise in switchgear is the influence of radiation. Radiation is difficult to estimate and are in some situations neglected. This makes the temperature rise simulations less accurate, as radiation can contribute with up to 40 % of the total power loss in an LBS, depending on the emissivity of the material and the temperature rise. [1]

The main purpose of this report is to use an existing MV switchgear unit and estimate how much of the power loss goes to thermal radiation. The result of this thesis will give a foundation for furthering the use of simulation to estimate the thermal radiation in other switchgear.

1.2 Objective

The objective of this report will be to estimate the how much of the power loss goes to thermal radiation in a MV switchgear unit with different load currents (temperature range), with both painted and non-painted current conductors.

This will include:

- Finding the the cold and warm resistance of the current path
- Finding the emissivity for the current path experimentally
- Estimating the surface area of the current path
- Preforming temperature rise test with the following loads:
 - o 630 A, 500 A, 400 A and 200 A
- Estimate the thermal radiation

1.3 Report structure

Chapter 1: Introduction

Chapter 2: Theory of the MV switchgear and the heat transfer mechanisms

Chapter 3: The MV switchgear test unit and the current source

Chapter 4: Estimation of the surface area of the current path

Chapter 5: Emissivity measurements on the current path using a thermal imager

Chapter 6: Resistance measurement of the current path and power loss estimations

Chapter 7: Temperature rise test with 630 A, 500 A, 400 A and 200 A load

Chapter 8: Thermal radiation estimate of each component in the current path at different loads

Chapter 9: The discussion

Chapter 10: The conclusion

2 Theory

This chapter explains the relationship between temperature and resistance and the different heat transfer mechanisms.

2.1 MV switchgear unit and RMU

MV switchgear is an important part of the power distribution, and often function as a connection between the distribution feeders and the power transformer. A MV switchgear unit can have a rated voltage up to 36 kV, a rated current up to 1250 A and can withstand short circuits up to 50 kA. [2]

A MV switchgear unit are usually found indoors and consist of a sealed tight metal enclosure which can contain; busbars, circuit breakers, fused switch disconnectors and contactors. It is also possible to include equipment who measure the current and voltage. The enclosure is often filled with insulating gas to avoid electrical discharge. Two gases who are commonly used are air and SF₆, where SF₆ are being phased out because of the negative impact it has on the environment. The insulating gas is chosen based on space requirements, reliability and availability, service requirements, operational safety, performance ratings. [2]

The RMU is a MV switchgear unit who can disconnect a faulted section in the distribution network and later reconnect the section, after the fault is corrected. This requires the MV unit to have feeding from two direction, see Figure 2.1. The rated voltage of an RMU MV switchgear unit is commonly up to 24 kV and the rated current is up to 630 A. A higher rated voltage requires higher pressure on the insulating gas. [2] [3]

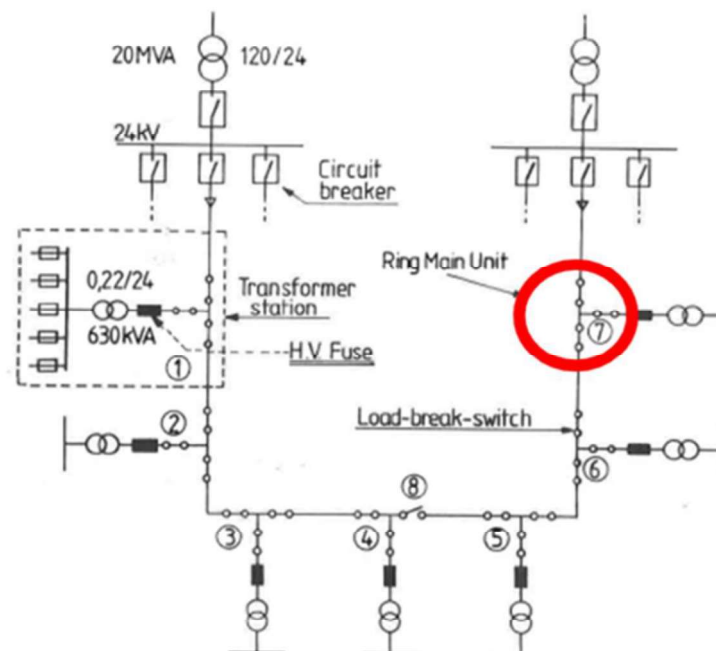


Figure 2.1: Ring feeding [3]

2.2 Power loss MV switchgear

Under operation of electrical equipment, the resistance in the current path will cause power loss. This power loss comes in the form of heat. The total power loss from the current path can be calculated using equation (2.1).

$$P_{tot} = R_{tot} * I^2 \quad (2.1)$$

P_{tot} = Power loss [W]

R_{tot} = Total resistance [Ω]

I = Current [A]

There are other sources to power loss, these includes the skin effect, eddy currents, proximity effect and more. These are not taken into account as the contribution of these seems to be insignificant when the current is below 1000 A. [4]

2.2.1 Resistance

The total resistance of the current path consists of the resistance in the bulk components and the resistance in the connections between the different components. Equation (2.2) shows how to calculate the total resistance in the current path. [3]

$$R_{tot} = R_{bulk} + R_{connection} \quad (2.2)$$

R_{tot} = Total resistance [Ω]

R_{bulk} = Total bulk resistance [Ω]

$R_{connection}$ = Total connection resistance [Ω]

2.2.1.1 The bulk resistance

The bulk resistance can be calculated using equation (2.3). The resistance of the bulk depends on length of the conductor, the specific resistance, the cross section of the conductor, the material and the production. The specific resistance is fundamental property of the material. [3]

$$R_{bulk} = \frac{l * \rho}{\sigma} \quad (2.3)$$

R_{bulk} = The total bulk resistance [Ω]

l = The length of the conductor [m]

ρ = The specific resistance [Ωm]

σ = Cross section of conductor [m^2]

The bulk resistance depends on the temperature, a change in temperature will change the bulk resistance. The change in bulk resistance can be calculated using equation (2.4).

$$R_{\vartheta} = R_0[1 + \alpha * \Delta T] \quad (2.4)$$

R_{ϑ} = The bulk resistance at temperature ϑ [Ωm]

R_0 = The bulk resistance at initial temperature, 20°C [Ωm]

α = The temperature coefficient [$1/^{\circ}\text{C}$]

ΔT = The temperature change [$^{\circ}\text{K}$] or [$^{\circ}\text{C}$]

2.2.1.2 Connection resistance

The resistance from the connections contributes often with substantial resistance. There are two types of connections stationary contacts and moving contacts. Stationary contacts are divided into two categories, non-separable like soldered, pressed or welded contact who are a rigid permanent joint, and separable contacts who can be separated, this category includes screwed and bolted contacts. Stationary contacts often have a lower resistance than moving contacts. Moving contacts are found in switches, and includes sliding contacts, rotating contacts and open/close contacts. The resistance for these connections depends on the quality and the category of the connection. [5]

For MV switchgear the connection resistance may contribute up to 20-40 % of the total power loss, depending on the number and type of contact used. [5]

Resistance in the connections are often greater than the bulk resistance because of the surface between the contacts. This surface is not uniform, but has many imperfections including surface film and unevenness. When the contact is exposed to voltage, the current will only flow through spots where there is metallic contact, these spots are called A-spots, see Figure 2.2. When the connection force increases, the area of the connection spot will also increase. Temperature can also affect the A-spots. [5]

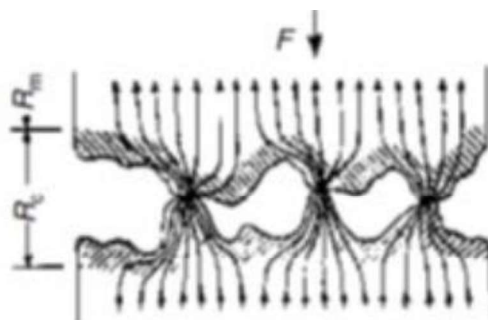


Figure 2.2: A-spot [5]

The resistance in the connection point depends on the temperature, but unlike the bulk resistance, estimating the resistance using the temperature is usually much more complicated.

Especially in moving contacts which consist of several components, where the different components affect each other.

2.3 Dynamic and stationary temperature rise

The total power loss in a MV switchgear unit comes in the form of heat and cause a temperature rise in the switchgear unit. Figure 2.3 shows the temperature rise at three different busbars with a load of 630 A. The busbars reach steady state after approximately 4-5 hours.

The figure is taken from the results of measurements using unpainted conductors done later in the report. The figure illustrates the typical temperature rise development.

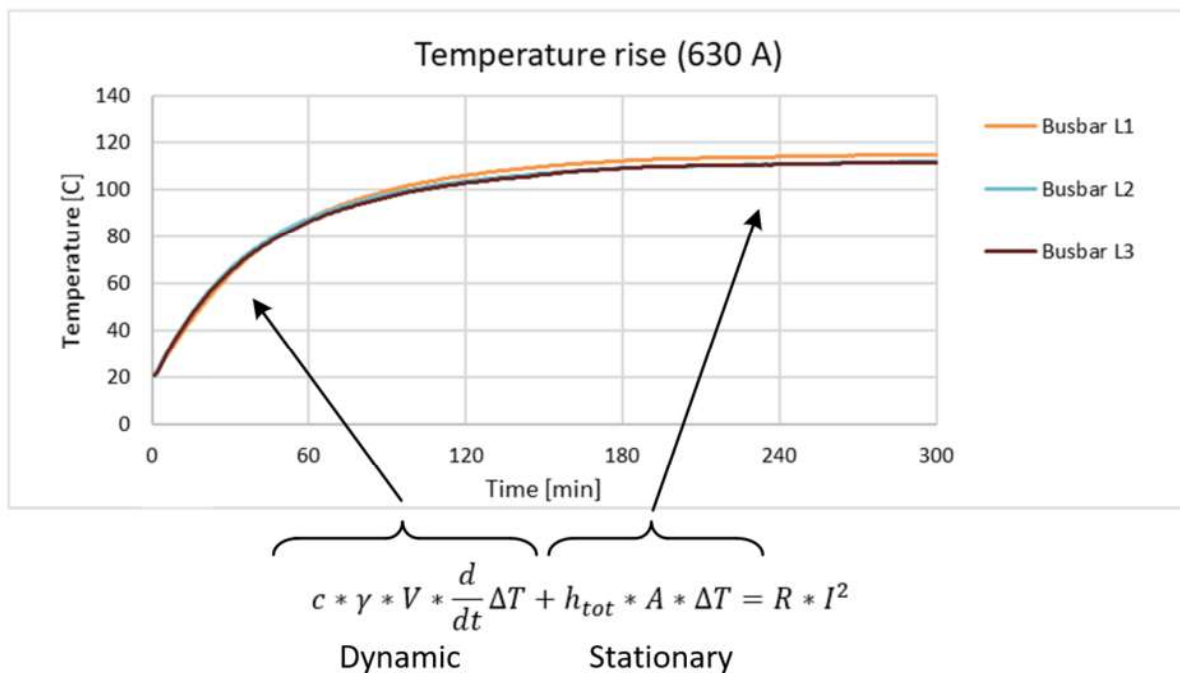


Figure 2.3: Dynamic and Stationary cases

Right after the power source is applied the temperature rises rapidly, this is called the dynamic phases, here the energy exchanged with the surroundings be neglected. The dynamic phases only last for a short amount of time before it is replaced by the stationary phase. The stationary phase is characterized by stabilization in the temperature. The temperature will continue to stabilize until it reaches steady state, defined as a temperature rise of less than 1 °C/hour. In the stationary phases there are no heat accumulated and all heat input are lost to the surroundings.

The temperature rise can be calculated using equation (2.5), which shows the relationship between the generated heat, the heat loss to soundings and the ohmic losses. Equation (2.5) includes both dynamic phenomena, and the stationary phenomena. This report will focus on the steady state temperature. [6] [7]

$$c * \gamma * V * \frac{d}{dt} \Delta T + h_{tot} * A * \Delta T = R * I^2 \quad (2.5)$$

C	= Specific heat [$J/(kg * ^\circ K)$]
γ	= Density [kg/m^3]
V	= Volume of conductor [m^3]
ΔT	= The temperature change [$^\circ K$] or [$^\circ C$]
h	= Heat transfer coefficient [$\frac{W}{m^2} * ^\circ K$]
A	= Surface area [m^2]
R	= Total resistance [Ω]
I	= Current [I]

2.3.1 Maximum temperature rise in switchgear

Degradation is often caused by high temperatures and may decrease the lifespan of the MV switchgear unit. Contact points in the current path is especially vulnerable for this, as the contact points often have a higher resistance than the bulk of the components, making the temperature rise highest in the contact points. When degradation takes place in a contact, the degradation will increase the resistance in the contact, making the temperature rise even higher. Some materials can withstand degradation more than others. [5]

The IEC has specified the maximum temperature rise in switchgear. These temperature limits are set to avoid degradation and depends on the material of the connection and the type of connection. These limits are given in “High-voltage switchgear and control gear, Part 1: common specifications” and are shown in Table 2.1. [5] [8]

Table 2.1: "Limits for temperature and temperature rise in air IEC table 3 [8]"

Nature of the part, of the material and of the dielectric air	Maximum value	
	Temperature [$^\circ C$]	Temperature rise at ambient air temp not exceeding $40^\circ C$ [K]
Spring loaded contacts		
Bare copper or bare-copper alloy contacts	75	35
Silver-coated or nickel coated contacts	115	75
Connections		
Bare-copper, bare-copper alloy or bare aluminium alloy	100	60
Silver coated or nickel coated	115	75

2.4 The Heat transfer mechanisms

Heat transfer is defined as transfer of thermal energy from a body of higher temperature to a body of lower temperature. The energy transfer only occurs because of the temperature difference between the bodies. As the thermal energy transfer over time is Joule/sec or watt, the thermal energy transfer will be calculated as power.

There are three main heat transfer mechanisms, conduction, convection and radiation. The total power for a system can be calculated using either equation (2.6). [7]

$$P_{total} = P_{cond} + P_{conv} + P_{rad} \quad (2.6)$$

P_{total} = Total power loss [W]

P_{cond} = Total power loss to conduction [W]

P_{conv} = Total power loss to convection [W]

P_{rad} = Total power loss to radiation [W]

Figure 2.4 shows how radiation, conduction and convection is transferred in an enclosure. The heat flow by conduction is transferred using the molecules within the bodies. The heat flow by convection is transferred using external motion. The heat flow by radiation is transmitted in electromagnetic waves between objects emitting and object absorbing the waves. [6] [7]

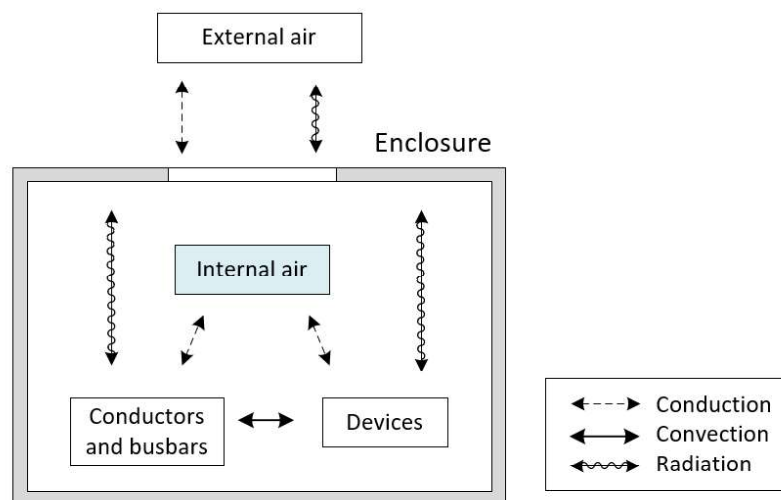


Figure 2.4: Heat transfer mechanisms [5]

2.4.1 Conduction

The first heat transfer mechanism is conduction. Conduction is characterized by direct contact between the medias in solid, liquid or gaseous bodies. The energy is transferred by motion in the molecules of the bodies. Electrons in metals are easy to move, making metals good conductors of both heat and electricity, showing the strong relationship between electrical and thermal conductivity.

2 Theory

The heat transfer by conduction can be calculated using equation (2.7). The thermal conduction is calculated by finding the temperature difference between two measuring points. [6] [7]

$$P_{cond} = \frac{\lambda}{L} * \sigma * \Delta T \quad (2.7)$$

- P_{cond} = Total power loss to conduction [W]
- σ = Cross section [m^2]
- λ = Thermal conductivity [$\frac{W}{m} \cdot ^\circ C$]
- l = Length between measuring points [m]
- ΔT = Temperature difference between the measuring points [$^\circ K$]

2.4.2 Convection

Convection is defined as heat is transferred by external motions in liquid or gas, the external motion can either be forced or natural. Natural or free convection means that the motion is caused by natural buoyance, like natural pressure difference. Forced convection includes applying something that will increase the gas flow, for instance a fan.

Convection can be calculated using equation (2.8). [6] [7]

$$P_{conv} = h_{conv} * A * (T_s - T_a) \quad (2.8)$$

- P_{conv} = Total power loss to convection [W]
- h_{conv} = Heat transfer coefficient convection [$W/m^2 * ^\circ K$]
- A = Surface transfer area [m^2]
- T_s = Surface temperature of conductor [$^\circ K$]
- T_a = Air temperature inside enclosure [$^\circ K$]

2.4.3 Radiation

Radiation is defined as transmission of heat by electromagnetic waves. All bodies with a temperature above absolute zero emit electromagnetic waves. Radiation does not need a transfer medium and can therefore also occur in vacuum. Thermal radiation depends on the material, and whether it can transmit electromagnetic waves or not. Liquids and solids can block the waves, even at very small thickness, $1 \mu m$ for metals and 1 mm for liquids. [9]

The electromagnetic wavelength transferring heat are usually between 0.8 and $400 \mu m$, which is found in the region of infrared light. This makes it possible to measure the radiation using a thermal imager which detects infrared light. Visible light has a wavelength of between 0.35 and $0.75 \mu m$, meaning that the human eye can see heat radiation, although this requires the radiation waves to be located within the range of the visible light. [6] [7] [9]

The heat transfer by radiation can be calculated using equation (2.9). The heat transfer depends on the emissivity of the body, the surface area, the temperature difference and the view factor. [6] [7]

$$P_{rad} = \varepsilon * \sigma_s * A * (T_s^4 - T_w^4) * f \quad (2.9)$$

- P_{rad} = Total power loss to radiation [W]
 ε = Emissivity of surface, between 0 and 1
 σ_s = Stefan Boltzmann's constant $5.67 * 10^{-8} \frac{W}{m^2 K^4}$
 A = Surface area of conductor [m^2]
 T_s = Surface temperature [$^{\circ}K$]
 T_w = Wall temperature [$^{\circ}K$]
 f = View factor, between 0 and 1

2.4.3.1 Emissivity

Emissivity ε or radiation ability is a body's ability to effectively emit thermal energy and are a value between 0 and 1. The value 1 is given to a perfect emitter or a black body emits 100 % of its the thermal energy. The value 0 is given to a body who emits 0 % of its thermal energy. The emissivity of some common materials is given in Table 2.2. [10] [11]

Table 2.2: Emissivity of common material [12]

Material	Emissivity
Aluminum polished	0.05
Aluminum oxidized	0.025
Copper, polished	0.02
Copper, oxidized	0.65
Electrical tape, black	0.95
Paint	0.94

The emissivity depends on the wavelength of the electromagnetic waves, the angle of emission, roughness, oxidation heat treatment and more. This can make it increasingly difficult to find the emissivity of a material, as a material can have several emissivity values depending on surface treatments. For metal, usually rougher oxidized surfaces have a higher emissivity than clean, polished, non-oxidized metal surfaces. [12] [13]

2.4.3.2 View factor

The view factor or shape factor is a geometric parameter who says something about how the objects surfaces are relative to each other.

The view factor has a value between 0 and 1. The value 0 is given to objects where the surfaces do not see each other. The value 1 is given to object where one of the objects encapsulates the other. A value between 0 and 1 given to surfaces that neither encapsulates each other or do not touch at all. When finding the view factor of an object, it is assumed that the radiation from the

2 Theory

object is uniform in directions in all directions, and that the medium between the objects don't affect, emit or absorbs the thermal radiation.

The view factor may be neglected in a simplified version of equation (2.9), instead it is assumed that 1 object encapsulates the other, such that the view factor is one, and is no longer necessary to include. [14]

3 System and equipment

This chapter focuses on the test device, the power source and the equipment.

3.1 The test device

The test device is a MV switchgear unit provided by USN and shown in Figure 3.1 and Figure 3.3, the full picture of the switchgear is shown on the front page. The test device is documents in the master thesis “Power loss measurements in MV switchgear for Cigré-working group” by Sandra Helland. [15]

Figure 3.1 shows the inside of the switchgear, where the back plate is removed. The isolation medium in the switchgear is air. The green cables fastened on different components and the inside and outside of the enclosure are thermocouple elements. The roof and the backside of the enclosure are the best cooling surfaces. The enclosure has double side walls. [15]

The listed parameters shows how the test device differs from a MV switchgear unit in operation:

- The lack of components in the test device, who support the current path and mechanisms who opens and closes the switches
- Only has four switches divided over three phases
- No connection to transformer, no current path and circuit breaker in the middle of the enclosure
- The switchgear enclosure unit in the test device is not sealed tight
- No additional cooling mechanism in the test device to decrease the temperature rise
- The initial temperature of the test unit was 20-22 °C, if the MV switchgear in operation differ from this it should be considered
- Low temperature rise in the input and high temperature in the output, impacts the heat distribution, and may cause degradation in especially vulnerable contacts

There are only four switches in the test device, under normal conditions there would have been six switches, two at each phase. This device has only four switches because the manufacturer produced only four switches, these switches was used in another experiment and after the experiment was done, they were given to USN. [15]

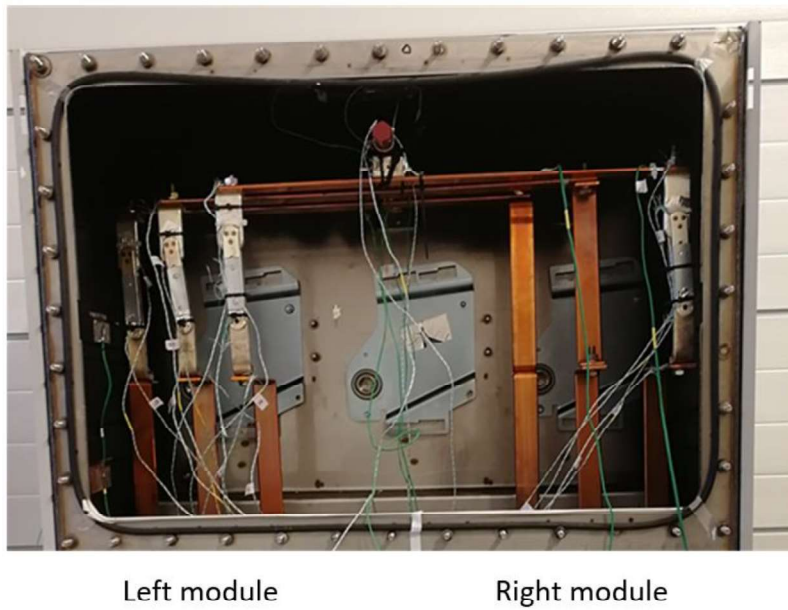


Figure 3.1: Switchgear, seen from the backside.

The current path of MV switchgear unit is show in Figure 3.2. The current path consists of several components, where the connection bars, the busbar and the replacements bar are made of copper, while the knife blade switches are made of silver coated copper

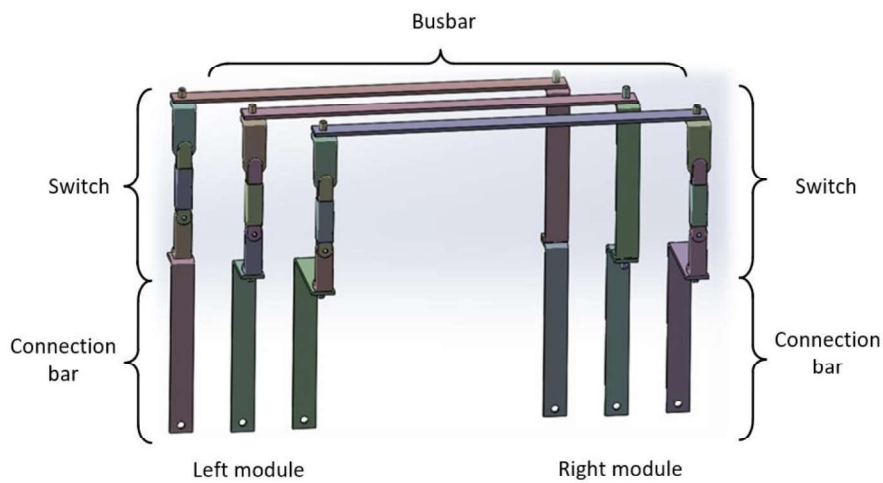


Figure 3.2 The current path

The bottom of the operating side of the switchgear is shown in Figure 3.3, illustrating the current input on the right module and the output on the left module where the current paths are short circuited

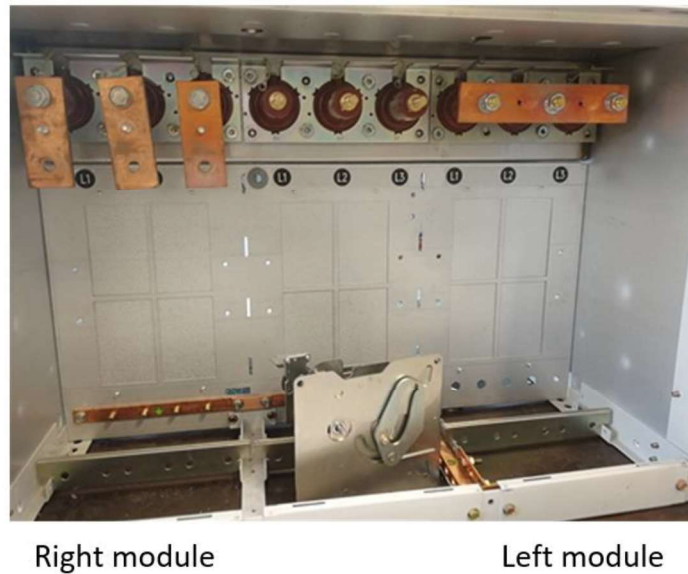


Figure 3.3: The current input on the right module and the current output on the left module, seen from the operating side

3.1.1 Paint

The first part of the experiment is done with unpainted conductors. Some of the walls are painted before the start of this project. The side walls, the roof and the removable back plate was painted with “Hot paint 650 °C” from Biltema. [16] The floor and the wall facing control panel in the enclosure is not painted. The current path is also unpainted.

The second part of the experiment is done with painted conductors, see Figure 3.4. “Hot paint 650 °C” from Biltema, which is a heat-resistant spray varnish used for painting surfaces that experience a high heat rise. The paint can withstand temperatures up to +650 °C and does not harden until the paint has warmed up. The purpose of this paint is to change the emissivity of the current path and to investigate the change in radiation. [16]

The current path has very little support, in terms of fastenings. Accidentally moving the parts of the current path will change the resistance of the current path, which can impact the radiation estimate. It is important to ensure that the current path is not moved under and after the current path is painted.

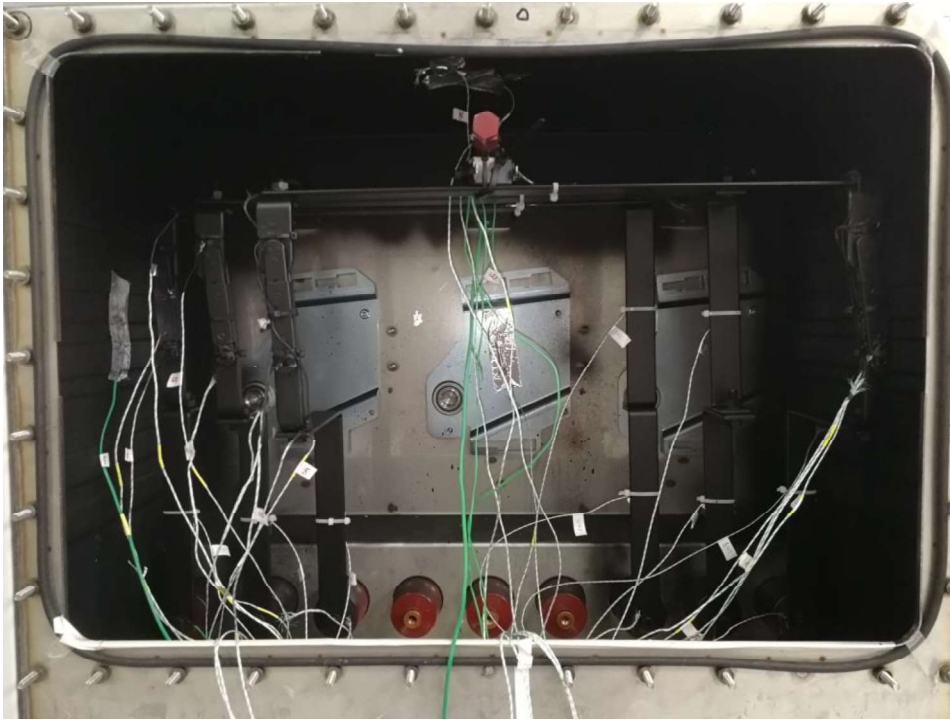


Figure 3.4: MV switchgear unit with painted current path

3.2 The equipment

The equipment used in this report is listed in Table 3.1 and are provided by USN. Following software was used in combination with the equipment; “SmartView 3.14” with the thermal imager reader, and “Agilent BenchLink Data Logger 3” to log the temperature measurements.

Table 3.1: Equipment list

Type	Manufacturer	Model
Thermal imager	Fluke	Ti25
Multiplexer	ABB	
Data acquisition/ switch unit	Keysight	34972A
Multimeter	Grossen Metrawatt	30M
Current injector tester	Hilkar	Ak23
Termocouple – Type K, class 1		

3.2.1 The current injector

The experiment conducted used a Hilkar current injector tester, see Figure 3.5, manufactured in 2014 as a power source. The current injector supply both AC and DC current. The DC output can deliver a current up to 100 A at a voltage between 0-13 V. The AC output used can deliver a current up to 2500 A at voltage of $3x\sqrt{3x(0 - 5)}$ V (ph-ph) and a frequency of 50 Hz according to the plate mounted on the current injector.

3 System and equipment



Figure 3.5: Hilkar current injector tester

4 Surface area estimation

This chapter contains the equipment, the procedure and the result for finding the surface area of the current path.

4.1 Equipment

To find the surface area of the current path a 3D model of the MV switchgear unit is used. The 3D model is given in Figure 4.1 and viewed in SolidWorks. Measurements of the different components are given Sandra Hellands master thesis “Power loss measurements in MV switchgear for Cigré-working group” and given in appendix C. These are used when manually calculating the surface area of the current path.

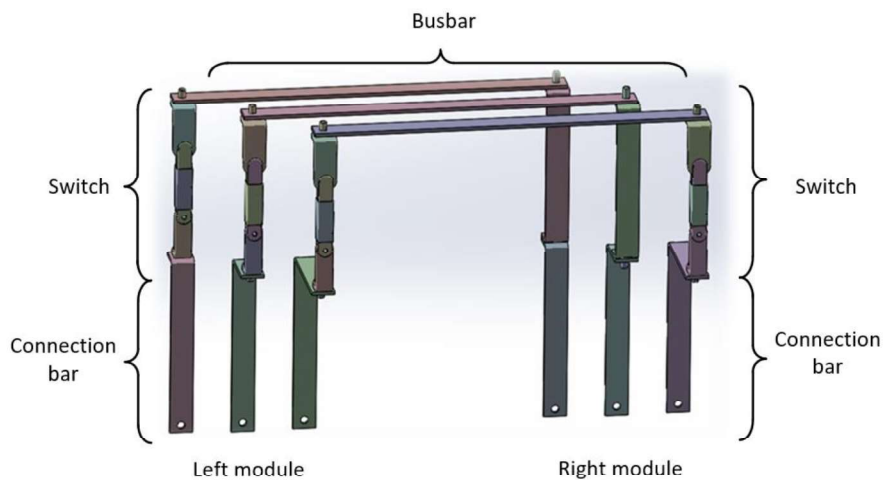


Figure 4.1: The current path of the MV switchgear unit

4.2 Procedure

SolidWorks makes it possible to find the surface area of every single surface on the 3D model, even curved surfaces, using the measurement tool. The surface on every component of the current path in the 3D model is added together and overlapping surfaces are subtracted to find the total surface which radiates thermal energy. Figure 4.2 shows the 3D model of one of the switches, where different parts of the switch are marked. The benefit of this method is that it is much easier to include all the curved surfaces in the calculation, these surfaces calculated with a bigger accuracy.

The surface area of the current path is also found by manually calculating the surface area, based on the measurements of the components in the current path. The downside of this method and the reason it is not used in the further calculation is the complexity of the switches, the overlapping area and the curvature, which makes the calculations less accurate.



Figure 4.2: The 3D model of the switches

4.3 Result

Result of the calculations of the surface area for both methods is given in appendix C. Table 4.1 shows the surface area of the current path using the 3D model. It is chosen to use the result from the 3D model in the thermal radiation estimate, after evaluating the accuracy.

This result using the 3D model is slightly higher than the result obtained using the measurements. This is most likely because the 3D model takes the curvatures and the complexity of the switches into account.

Table 4.1: Surface area of current path using the 3D model

Surface area [m ²]					
	Connection bar	Switch	Busbar	Switch/replacement bar	Connection bar
L1	0.0436	0.0289	0.0597	0.0289	0.0436
L2	0.0346	0.0289	0.0597	0.0337	0.0346
L3	0.0300	0.0289	0.0597	0.0337	0.0300

5 Emissivity measurements

This chapter contains the equipment, the procedure, the result and the discussion for finding the emissivity of the current path.

5.1 Equipment

To find the emissivity of the current path, following equipment has been used; a thermal imager of type Ti25, se Figure 5.1, with IR fusion technology from Fluke, thermocouple elements of type K and different types of masking and electrical tape. The software SmartView[®] is used to process the images taken with the thermal imager. [11]



Figure 5.1: The thermal imager from Fluke

The thermal imager converts infrared radiation to temperature measurements. The accuracy of the thermal imager is $\pm 2\text{ }^{\circ}\text{C}$ or 2 % (whichever is greater) and will depend on the emissivity of the material. Material with higher emissivity like painted metal, wood or masking tape gives very accurate measurements. This is because these types of material radiates a lot of thermal energy for the thermal imager to detect. Materials with high emissivity can often use values given in the emissivity tables. [11] [12]

Material with low emissivity, like polished aluminium or polished copper radiates less energy for the thermal imager to detect, they can be difficult to find in tables as they depend on the surface treatment of the material. It is often necessary to find them experimentally to get accurate temperature measurements using the thermal imager. [11] [12]

5.2 Procedure

There are two common methods to determine the emissivity of a material, using a thermal imager. The back wall on the MV switchgear unit is removed during the emissivity measurements to get access to the current path. [12]

5.2.1 Method 1: Thermocouple elements

Thermocouple elements are fastened on the current path facing the operating side of the MV switchgear unit using aluminum tape, see Figure 5.2. This is to give a larger area to measure the emissivity on as the emissivity is measured on the current path, on the side facing the backwall.



Figure 5.2: Thermocouple elements fastened to the backside of the current path

The current path is then heated with 630 A current in approximately 1 hour until the temperature is somewhat steady. The thermal imager is pointed towards the copper bar or switch to measure its emissivity. The emissivity of the thermal imager is changed until the temperature of the thermal imager matches the temperature found by the thermocouple elements, see Figure 5.3. This will be done on several of the copper bars to find an average emissivity for the copper and then on several of the switches to find the average emissivity of silver coated copper. [12] [17]

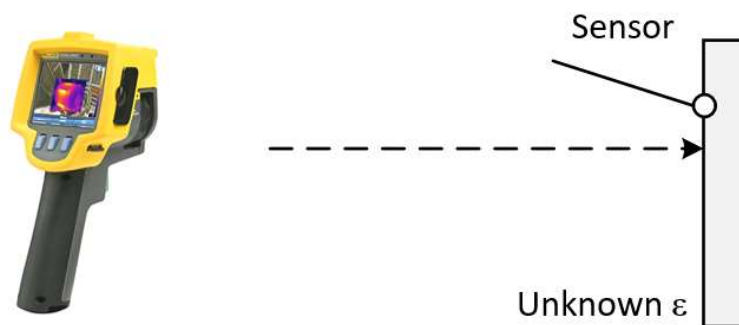


Figure 5.3: Emissivity measurements using thermocouple elements [18]

5.2.2 Method 2: Tape

Masking tape and/or electrical tape are fastened the copper bars on the side facing the back wall. The tape should cover no more than half the copper bar, such that there are enough space to both measure the emissivity of the copper and the temperature of the tape on the copper bar, see Figure 5.4. The thermocouple elements fastened facing on the operating side of the copper bars is not removed, these are not necessary for the method, but are used to verify the result.

5 Emissivity measurements



Figure 5.4: Finding the emissivity using three different type of tape

A 630 A current is applied for about 1 hour. The thermal imager's emissivity is set to $\epsilon = 0.95$, and the temperature of the tape is measured. This temperature is compared to the thermocouple elements to verify that the tapes have an emissivity of 0.95. Then the thermal imager is directed to the part of the conductor which is not covered by tape. The emissivity of the thermal imager is then changed until the temperature given by the thermal imager matches the temperature found previously on the tape, see Figure 5.5. Several measurements will be taken and an average for the different material will be found. This method should only be used on objects heated to a temperature lower than 100 °C. [12] [17]

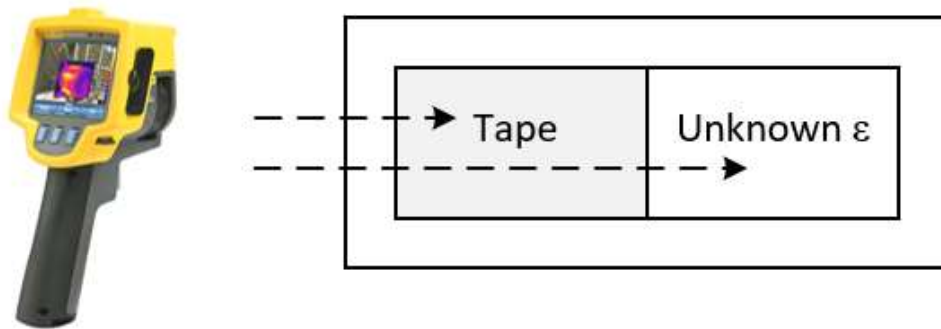


Figure 5.5: Finding the emissivity using tape [18]

5.3 Result

The thermal images of one copper bar and one switch are given in Figure 5.6. These images are taken with the correct emissivity value for the materials. The temperature range of the thermal imager is different in the two images.

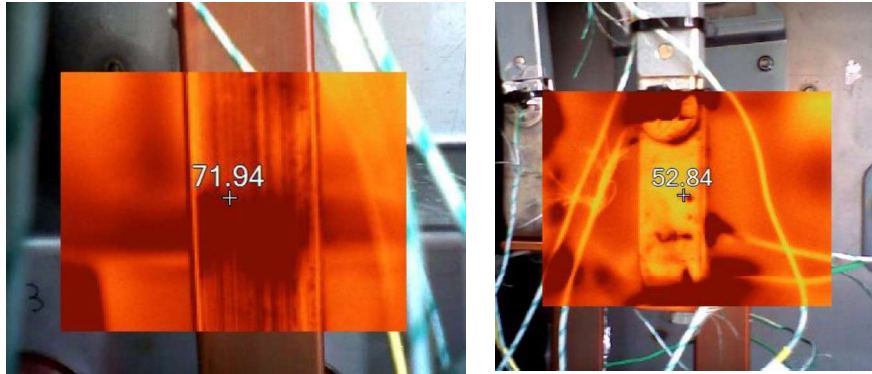


Figure 5.6: Thermal image of the copper bar and the switch

The final emissivity values for the different materials are given in Table 5.1 and in appendix D. The copper components are the only value who is found both by using thermocouple elements and tape. This is because they were the only component with a large enough surface to properly measure both the temperature on the tape and emissivity of the material. The emissivity of the masking tape and the electrical tape was done using thermocouple elements. This was to make sure that the emissivity of the different types was 0.95, as they had very different surface.

After the conductors were painted the emissivity of the paint was measured using thermocouple elements. This was done after all the temperature, resistance and emissivity measurements for the unpainted conductors were done.

Table 5.1: The emissivity results

Placement	Emissivity
Switches (Silver coated copper)	0.10
Copper components	0.22
Copper components (using masking tape)	0.21
Painted conductor	0.93
Masking tape/ electrical tape	0.95

The emissivity of the painted conductor and the masking electrical tape are approximately the same as the values given in Table 2.2 The emissivity of copper and silver coated copper components are lower than in the thesis “Heat transfer mechanisms in MV load break switches” by Stein Øygarden, who estimated 0.17 for silver coated copper and 0.27 for copper. [19] Emissivity of materials with low emissivity depends a lot on the surface treatment of the material. Copper from instance can vary between 0.02 and 0.65 depending on whether material is polished or oxidized. The emissivity result can therefore be assumed to be within acceptable limits.

6 Resistance measurement and power loss estimation

This chapter contains the equipment, the procedure, the result of the resistance measurements and the power loss estimate.

6.1 Equipment

To measure the warm and the cold resistance following equipment have been used: METRA HIT true RMS multimeter and datalogger, thermocouple elements and a measuring box for finding the resistance of a components between two thermocouple elements. The equipment is shown in Figure 6.1.

The resistance is partly measured directly on the current path, and partly by using thermocouple elements. Resistance measured using thermocouple elements is particularly useful when the measurements cannot be done directly on the current path. For instance, during the temperature rise test on the MV switchgear unit when the back plate is mounted. The resistance of a component is then found by measuring the voltage drop between two thermocouple elements. The thermocouple elements and the multimeter can be plugged into the measuring box to make the measuring process easier.



Figure 6.1: METRA HIT multimeter, thermocouple element and a measuring box

6.2 Procedure

The purpose of finding the resistance of the current path is to estimate the total power loss in the enclosure. The resistance in the components changes with the temperature, see equation (2.3), such that both cold and warm resistance for the components should be found at the different loads.

6.2.1 Cold resistance

The cold resistance is measured with a 100 A DC current load applied, as this current magnitude is not high enough to heat the current path. A DC current is used to only measured the resistive component of the impedance, and not the inductive or capacitive component. The

6 Resistance measurement and power loss estimation

METRA HIT multimeter is then used to measure the voltage drop directly over each component, and across each phase and over three of the switches using thermocouple elements. The cold resistance is calculated using the injected current magnitude and the measured voltage drop.

6.2.2 Warm resistance

The warm resistance is measured after the temperature of the current path has reached steady state at a chosen load. To measure the resistance the AC source is disconnected and a 100 A DC source is connected. The voltage drop will be measured across each phase and over three of the switches using thermocouple elements.

When the DC source are connected the temperature will fall drastically, it is therefore important to do the temperature measurements as quickly as possible. The temperature measurements are done within 5 minutes, phase L1 and L2 are measured first and phase L3 is measured last.

6.3 Result

The result of the resistance and power loss measurements included the resistance in the switches and the bolts are given in this sub-chapter.

6.3.1 The cold resistance of the components

Table 6.1 shows the cold resistances for the different components with unpainted conductors compared to previous measurements done on the same MV switchgear unit in Sandra Helland master thesis. [15]

Table 6.1: Current and previous measured cold resistance of the current path

	Module	L1 [$\mu\Omega$]		L2 [$\mu\Omega$]		L3 [$\mu\Omega$]	
		Measured resistance	Resistance from [15]	Measured resistance	Resistance from [15]	Measured resistance	Resistance from [15]
Connection bar*	Left	35.8	37.7	29.8	28.7	30.1	22.9
Switch	Left	41.3	48.8	49.6	47.5	38.6	48.0
Busbar*		50.4	48.8	48.4	47.9	50.1	48.6
Switch/replacement bar	Right	39.9	48.2	21.8	26.2	21.1	25.9
Connection bar*	Right	36.7	36.3	27.8	26.1	23.8	23.1
Sum resistance		204.1	219	177	176	164	168

*Includes the contact resistance on both sides

Table 6.1 shows the difference between measured resistance and previous measured resistance. The measurements are close to each other, but there are also several differences. The measurements are taken using the probes from the METRA HIT multimeter directly on the current path, this can explain the variation in the connection bars, busbars and the replacement bars, as it is difficult to know where on the end of the components the previous measures have

6 Resistance measurement and power loss estimation

been measured. The current path can also easily have been moved which will impact the switches the most.

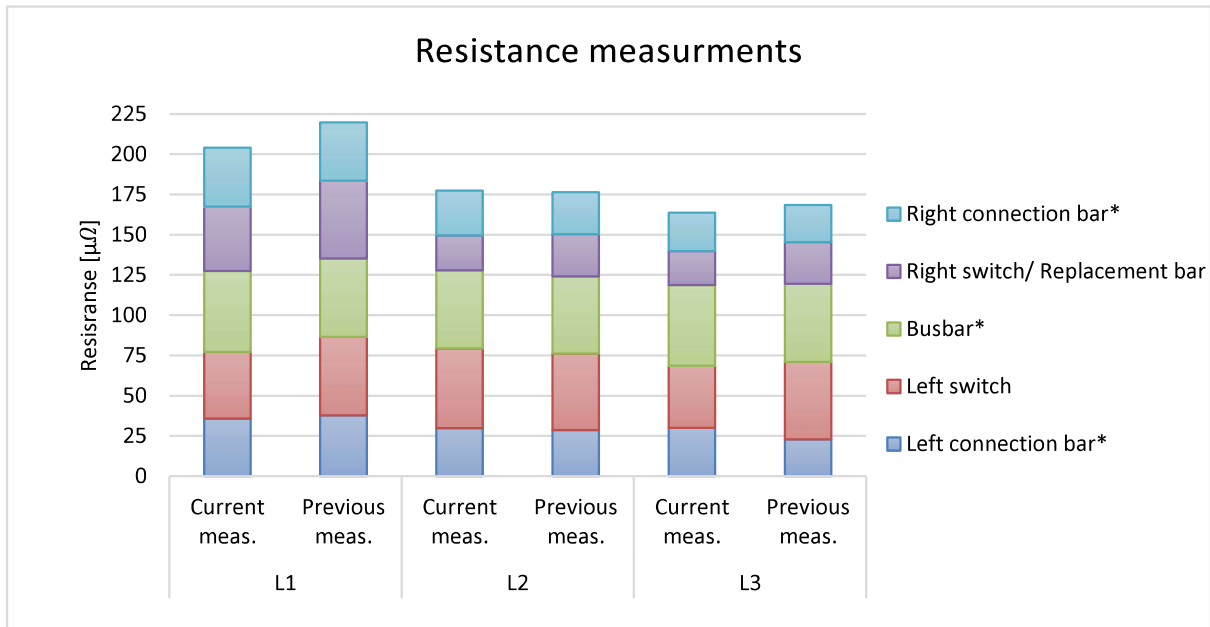


Figure 6.2: Cold resistance comparison

Figure 6.2 illustrates the difference between the current and the previous measurements on the same MV switchgear unit, using the values found in Table 6.1. The largest difference between the current and previous measurements is found in phase L1. This is easily explained, as L1 has two switches which can very easily be moved and change in resistance. The resistance in L3 and L3 are lower as they only have one switch. The measured values from the cold resistance is found to be within acceptable limits and the current measurement for phase L1 will be used in power loss estimations.

6.3.2 The warm resistance for the phases

The warm resistance and cold resistance for phase L1, L2 and L3 for unpainted and painted conductors are shown in Table 6.2 and Table 6.3. The values are found using thermocouple elements, with different current loads.

Table 6.2: The resistance at different load currents with unpainted conductors

Phase	Total resistance unpainted [$\mu\Omega$]				Cold resistance
	Warm resistance (At steady state)				
	630 A	500 A	400 A	200 A	
L1	238	233	212	202	192
L2	217	193	183	170	163
L3	182	176	171	165	156

6 Resistance measurement and power loss estimation

Table 6.3: The resistance at different load currents with painted conductors

Total resistance painted [$\mu\Omega$]					
	Warm resistance (At steady state)				Cold resistance
Phase	630 A	500 A	400 A	200 A	
L1	251	231	220	207	197
L2	222	198	190	170	174
L3	177	174	169	164	161

Table 6.2 and Table 6.3 shows that the resistance increases when the temperature of the current path increases. The resistance in the unpainted and painted conductors are different. The total resistance in phase L1 is for instance higher with painted conductors, while phase L1 is lower for painted conductors. This can be due to the painting process, where some of the components may have been moved, or because of the paint itself.

Figure 6.3 shows the cold and warm resistance at different load currents with painted and unpainted conductors.

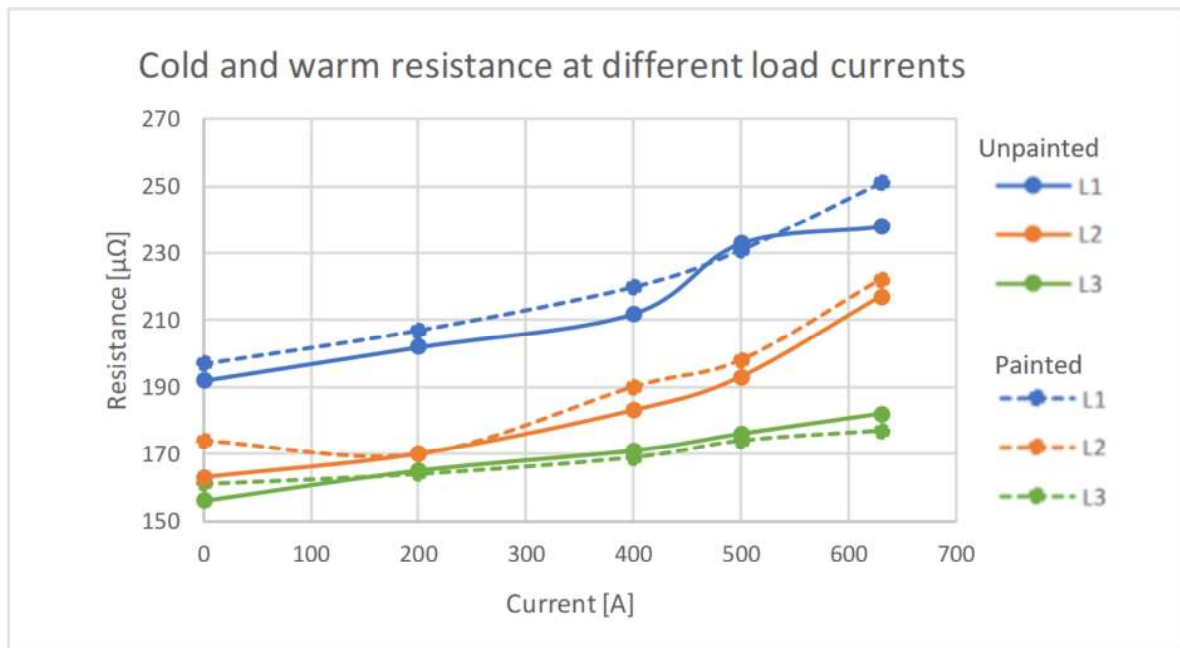


Figure 6.3: Total warm resistance for each phase

Figure 6.3 shows that the resistance in phase L1 and L2 is higher with painted conductors, but for phase L3 the unpainted conductors have a slightly higher. Both unpainted and painted conductors follows the same slope for each of the phases. Some of the values differs more than other, these can be the result of repeatedly heating and cooling the switchgear unit. In conclusion the cold and warm resistance of the painted and unpainted conductors are within acceptable limits.

6 Resistance measurement and power loss estimation

6.3.3 The warm resistance in the copper bars

Only the cold resistance of the copperbars and the busbar in phase L1 have been experimentally measured. The warm resistance of the copperbars are estimated using equation (2.4), the cold resistance values from Table 6.1, a temperature coefficient of 0.00386 for copper and temperature rise measurements from Table 7.1 and Table 7.2.

The estimated warm resistance for phase L1 with both painted and unpainted copper conductors is given in Table 6.4 and Table 6.5.

Table 6.4: Cold and estimated warm resistance for connection bar and busbar for phase L1 unpainted

Resistance copper components L1 unpainted [$\mu\Omega$]					
	Warm resistance (At steady state)				Cold resistance
	630 A	500 A	400 A	200 A	
Connection bar – L	48.1	44.0	41.0	37.6	35.8
Busbar	68.6	62.6	58.2	52.9	50.4
Connection bar – R	45.9	42.9	40.5	38.0	36.7

Table 6.5: Cold and estimated warm resistance for connection bar and busbar for phase L1 painted

Resistance copper components painted [$\mu\Omega$]					
	Warm resistance (At steady state)				Cold resistance
	630 A	500 A	400 A	200 A	
Connection bar – L	47.0	43.6	40.9	37.5	35.8
Busbar	63.9	59.6	56.5	52.4	50.4
Connection bar – R	45.1	42.2	40.1	37.9	36.7

Both Table 6.4 and Table 6.5 uses the same cold resistance. This is because the paint layer made it difficult to measure the resistance over each component using measurement probes. The differences between the painted connection bars and the unpainted are solely because of the difference in temperature rise values. All the copper bars are bulk components, which equation (2.4) requires for good estimations. The estimated results are within expected limits

Figure 6.4 shows the estimated warm resistance and the cold resistance for the copper components in phase L1.

6 Resistance measurement and power loss estimation

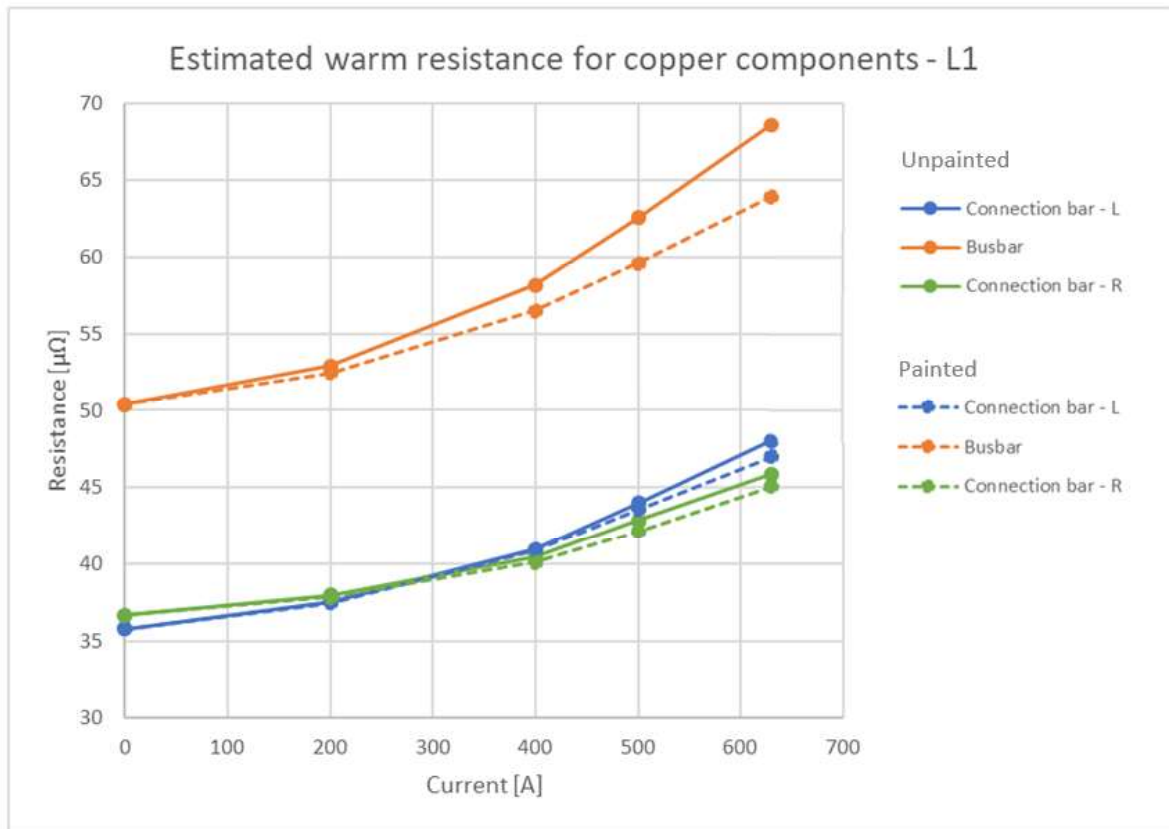


Figure 6.4: Warm resistance for copper components phase L1 unpainted

Figure 6.4 shows how the different temperature values affect the estimation of the copper bars. The temperature rise for unpainted conductors is higher than for painted conductors, making the warm resistance for the unpainted conductors higher. This is especially visible on the busbar. Both the connection bars on the right module and the left module follow the same slope, this is expected as the connection bars are identical components.

6.3.4 The warm resistance in the switches

To show that the resistance of the switches often are difficult to estimate, the measured warm resistance are compared to an estimate of the warm resistance, to see how they differed from each other.

6.3.4.1 Unpainted conductors

The warm resistance of the unpainted switches are measured using thermocouple elements. The switches are also estimated using equation (2.4), a temperature coefficient of 0.00386, the warm resistance is found in Table 6.1 and a temperature rise found in Table 7.1.

Table 6.6 shows the measured and estimated warm and cold resistance when the switches are unpainted.

6 Resistance measurement and power loss estimation

Table 6.6: The warm and cold resistance for the switches when unpainted

		Warm resistance (At steady state) [$\mu\Omega$]				Cold resistance [$\mu\Omega$]
	Switch	630 A	500 A	400 A	200 A	
Measured	L1 – L	42.2	40	38.8	37.8	35.5
	L1 – R	46.2	44.1	40.0	39.7	37.3
Estimated	L1 – L	49.1	44.6	41.4	37.3	35.5
	L1 – R	50.6	46.1	43.0	39.1	37.3

The warm resistance for the unpainted switches increases as the temperature increases. The estimated values increase more than the measured values.

Figure 6.5 shows the resistance at different temperature rise values and uses values from Table 6.6.

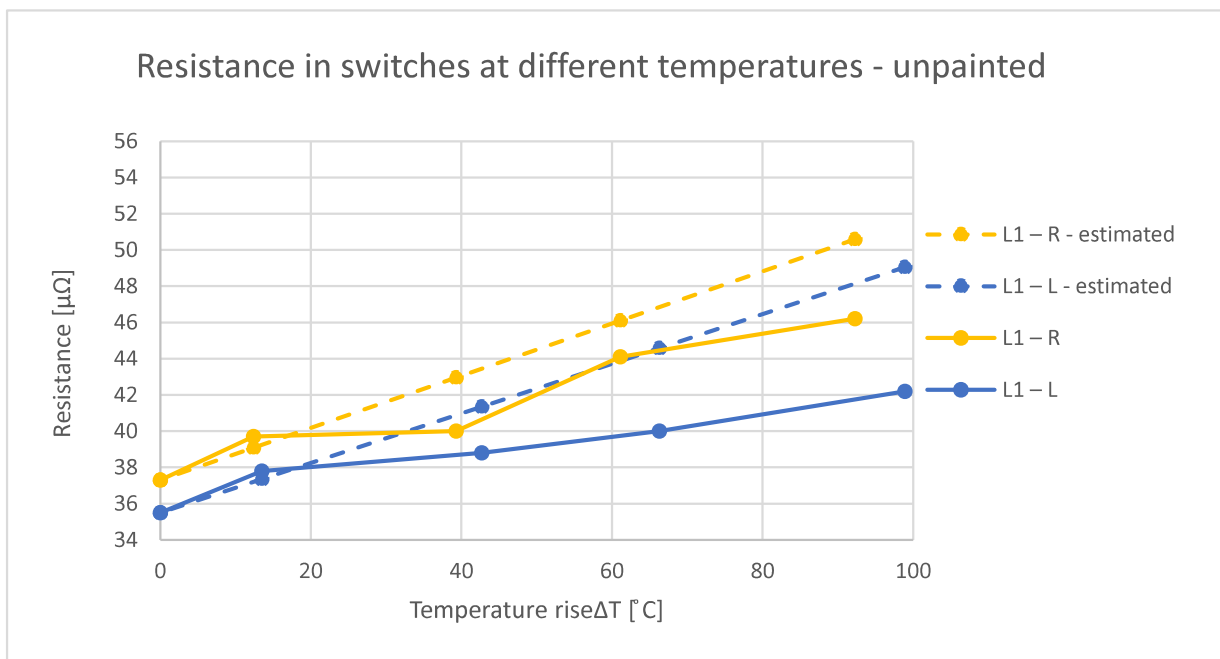


Figure 6.5: The change in the resistance of the switches with temperature rise unpainted

Figure 6.5 shows that there are significant difference between the measured and the estimated resistance of the switches. The difference is small for 200 A but increases in size as the current load increases. The higher the current the larger deviation. It can be concluded that the switch is far too complicated and consist of too many components and connection points to be calculated using equation (2.4), which are meant for bulk resistances, for higher temperature rise values.

6.3.4.2 Painted conductors

The warm resistance of the unpainted switches are measured using thermocouple elements. The switches are also estimated using equation (2.4), a temperature coefficient of 0.00386, the warm resistance if found in Table 6.1 and a temperature rise found in Table 7.2.

6 Resistance measurement and power loss estimation

Table 6.6 shows the measured and estimated warm and cold resistance when the switches are unpainted.

Table 6.7: The warm and cold resistance for the switches when painted

		Warm resistance (At steady state) [$\mu\Omega$]				Cold resistance [$\mu\Omega$]
	Switch	630 A	500 A	400 A	200 A	
Measured	L1 – L	41.6	39.4	39.7	38.8	36.5
	L1 – R	49.7	45.6	44.1	42.7	43.0
Estimated	L1 – L	47.8	44.3	41.8	38.1	36.5
	L1 – R	54.2	50.7	48.0	44.7	43.0

The warm resistance for the unpainted switches increases as the temperature increases. The estimated values increase more than the measured values.

Figure 6.6 shows the resistance at different temperature rise values and uses values from Table 6.7.

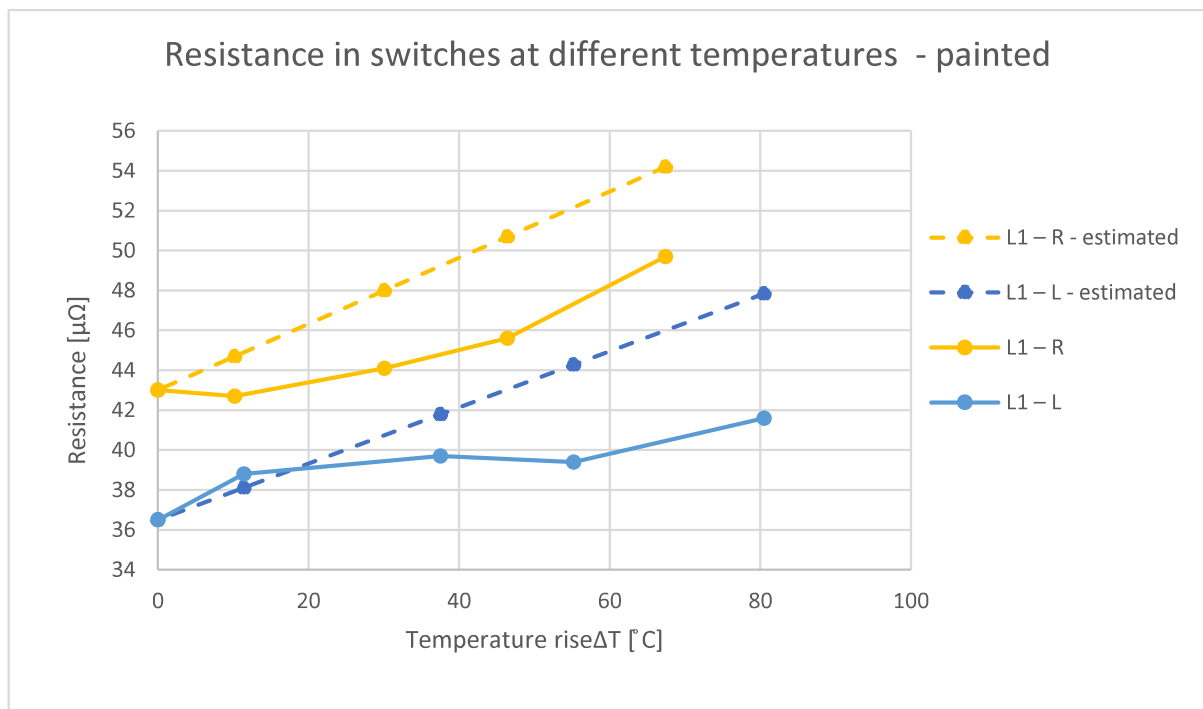


Figure 6.6: The change in the resistance of the switches with temperature rise painted

Figure 6.6 shows that the estimated resistances increases faster than the measured resistances for the painted switches. The difference increases with the temperature rise. It can again be concluded that equation (2.4), is not suitable for estimating the warm resistance for switches with high temperature rise. The switches are far too complicated to be considered a bulk resistance, which equation (2.4) requires for accurate estimated resistances.

6.4 Estimated power loss

The total power loss of each of the phases in the MV switchgear unit are calculated using equation (2.1) at different current loads, with painted and unpainted conductors. Table 6.8 shows the total power loss using measured resistance values from Table 6.2 and Table 6.3.

Table 6.8: Power loss estimate using measured values

Phase	Unpainted [W]				Painted [W]			
	630 A	500 A	400 A	200 A	630 A	500 A	400 A	200 A
L1	95	58	34	8	100	58	35	8
L2	86	48	30	7	88	50	30	7
L3	72	44	27	7	70	43	27	7
Total	252	150	91	22	257	150	93	22

Table 6.8 shows that the power loss is highest in phase L1, which has two switches. The power loss increases with the current load and the power loss in the painted conductors are slightly higher than the unpainted conductors.

Figure 6.7 shows the total power loss at different load currents using values from Table 6.8.

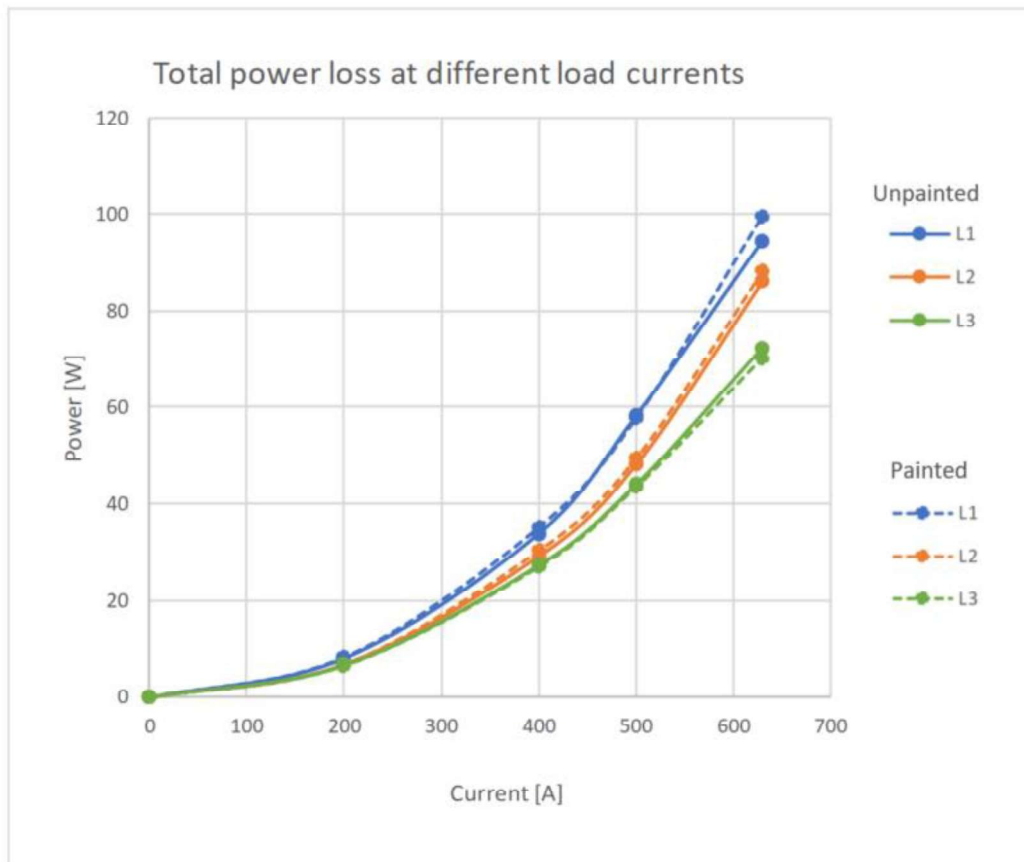


Figure 6.7: Total power loss at different load currents

6 Resistance measurement and power loss estimation

Figure 6.7 shows that the power loss with the unpainted conductors are almost identical to the power loss with unpainted conductors. It can be concluded that painting the conductor did not drastically affect the power loss. from Table 6.2 and Table 6.3.

Table 6.8 and Figure 6.7 differs substantially from the power loss estimate on the same test unit done in the master thesis “Power loss measurements in MV switchgear for Cigré-working group”. In the master thesis the power loss includes the connections on the input and output of the current path. While the power loss in Table 6.8 only includes the current path physically inside the enclosure and not the current input on the bolts and washers. [15]

6.4.1 The power loss for each component in phase L1

The total power loss form each component are calculated using the estimated warm resistance of the copper bars from Table 6.4 and Table 6.5 and the measured warm resistance of the switches from Table 6.6 and Table 6.7.

The power loss for each component in phase L1 for both painted and unpainted conductors are given in Table 6.9.

Table 6.9: Power loss for phase L1 estimate using estimated values

	Unpainted [W]				Painted [W]			
	630 A	500 A	400 A	200 A	630 A	500 A	400 A	200 A
Connection bar	19	11	6.6	1.5	19	11	6.5	1.5
Switch	17	10	6.2	1.5	17	10	6.4	1.6
Busbar	27	16	9.3	2.1	25	15	9.0	2.1
Switch/ replacement bar	18	11	6.4	1.6	20	11	7.1	1.7
Connection bar	18	11	6.5	1.5	18	11	6.4	1.5
Total	100	58	35	8.2	98	58	35	8.4

The total estimated power loss for each component in phase L1 given in Table 6.9 are almost identical to the measured power loss in phase L1 in Table 6.8. On the background of this, it can be concluded that the estimated resistances for the copper bars are within acceptable limits, and that the power loss of each component with painted and unpainted conductors at different loads are accurate.

7 Temperature rise test

This chapter contains the equipment, the procedure and the result of the temperature rise tests.

7.1 Equipment

To find the temperature of the current path and on the enclosure, following equipment has been used; thermocouple elements, a multiplexer, a data acquisition/switch unit and the computer program “Agilent BenchLink Data Logger 3”.

The thermocouple elements are of type K, and has an accuracy of $\pm 0,004t$ or $\pm 1,5^{\circ}\text{C}$. The thermocouple elements are plugged into the multiplexer who transfers the data to the data acquisition/switch unit. The multiplexer and the data acquisition/switch unit are shown in Figure 7.1. The temperature values are logged using the computer program “Agilent BenchLink Data Logger 3”.

There are 40 thermocouple elements fasten on the current path and inside and outside of the enclosure. 32 of the sensors were already there, as they were used in previous experiments. 8 sensors were added to the middle of the connection bars and the replacement bars. The full list of thermocouple elements is given in appendix B. The thermocouple elements are fastened using aluminium tape and strips or under the washers beneath the bolts on the current path.



Figure 7.1: The temperature logging devises

7.2 Procedure

The temperature measurements are done for the following current loads: 630 A, 500 A, 400 A and 200 A. The temperature is measured from the load is applied to the temperature has reached steady state, this takes between 4-5 hours. The temperature is logged every minute. The most important temperature values are the initial temperature, the steady state temperature and the temperature rise.

7.3 Result

The result of the temperature rise measurements are given in appendix F, which includes the initial temperature, the steady state temperature and the temperature rise for all the sensor for 630 A, 500 A, 400 A and 200 A loads with both painted and unpainted conductors.

The temperature measurements presented in this sub-chapter are taken with sensors who can best represent the temperature of the whole components. Therefore the temperature is measured on the middle of the copper bars, and not in the contacts. Only the switches are measured in the contacts, such that only they are restricted by the temperature limits set by IEC. The measurements from the other contacts in the current path is available in appendix F. The temperature rise values for phase L1, L2 and L3 is given in appendix E.

7.3.1 Unpainted

Figure 7.2 shows the temperature rise in phase L1 at the different load currents when the current path is unpainted.

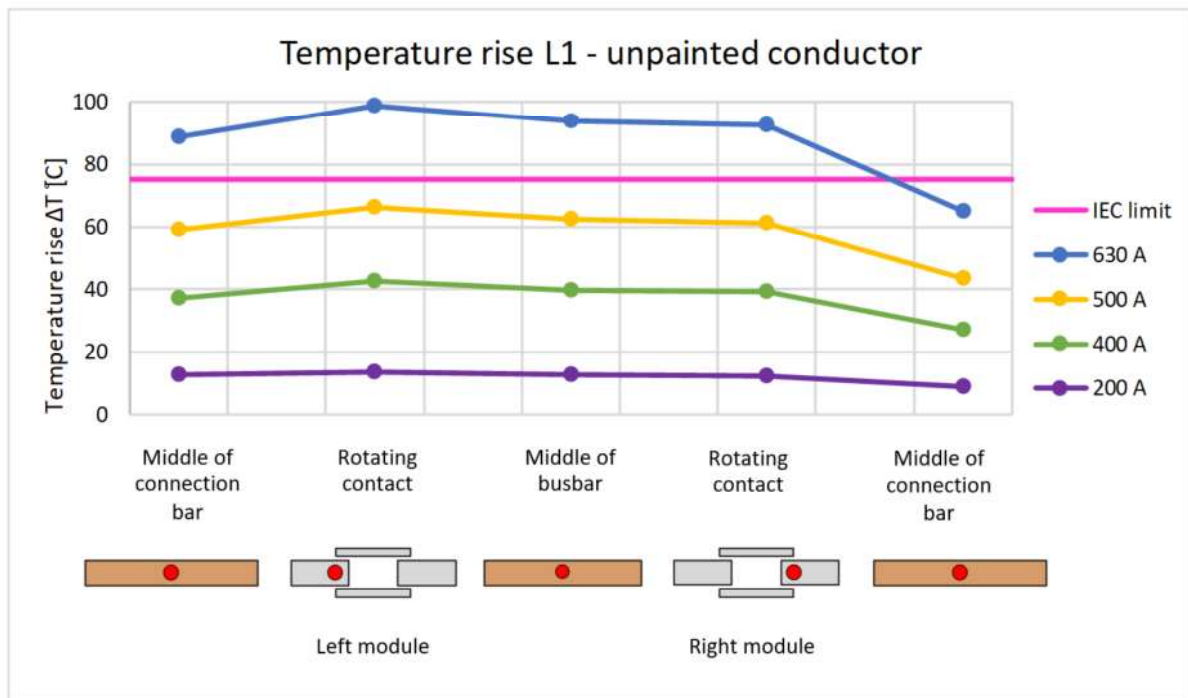


Figure 7.2: The temperature rise of phase L1 when unpainted

Figure 7.2 shows that the warmest point on the current path is on the rotating contact on the left module and that the lowest temperature is on the middle of the connection bar on the right module. The reason for the low temperature on the brushing connection on the right module is that the heat escapes through the current input. The maximum temperature rise is 75 °C for silver coated spring-loaded. Figure 7.2 shows that the load of 500 A is within the maximum temperature rise limits set by IEC.

Table 7.1 shows the temperature rise at different load currents with unpainted current path.

7 Temperature rise test

Table 7.1: The temperature rise at different load currents with unpainted current path

Sensor	Placement	Temperature rise ΔT [°C]			
		630 A	500 A	400 A	200 A
Phase L1					
40	Middle of connection bar	88.8	59.3	37.4	12.7
3	Rotating contact – left	98.9	66.3	42.7	13.5
6	Middle of busbar	93.7	62.5	39.9	12.9
9	Rotating contact – right	92.3	61.1	39.3	12.4
41	Middle of connection bar	64.9	43.7	26.9	9.1
Enclosure surface					
23	Middle of inside, side wall	18.9	12.6	6.9	2.7
26	Middle of inside, top surface	20.5	14	7.9	3.2

This is confirmed in Table 7.1, who contains the temperature rise values used in Figure 7.2. The colour green used on the table indicates the temperature measurements on the switches that are within IEC limits. Table 7.1 shows that switches are within IEC temperature rise limit with 500 A, 400 A and 200 A current load.

7.3.2 Painted

Figure 7.3 shows the temperature rise in L1 at different load currents with painted current path.

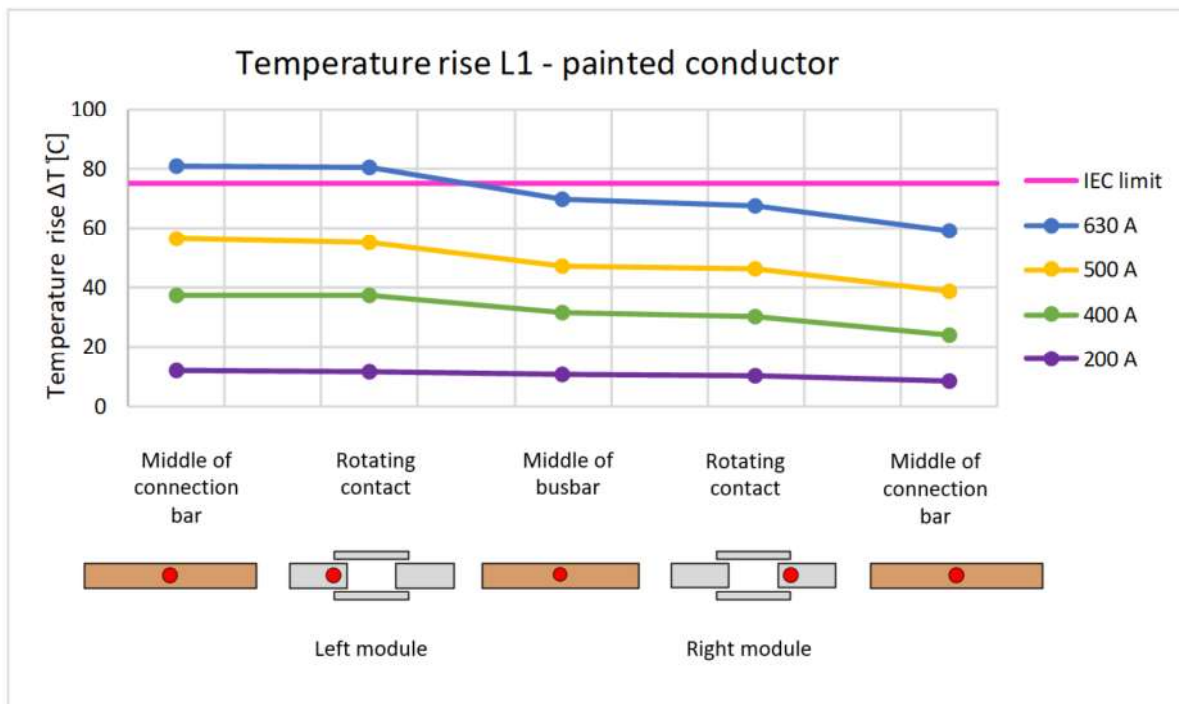


Figure 7.3: The temperature rise of phase L1 when painted

7 Temperature rise test

Figure 7.3 shows that the warmest point on the current path is on the middle of the connection bar on the left module as the current output on the left module is short circuited. The lowest temperature is on the middle of the connection bar on the right module. The reason for the low temperature on the brushing connection on the right module is that the heat escapes through the current input. The maximum temperature rise is 75 °C for silver coated spring-loaded contacts. Figure 7.3 shows that the load of 500 A is within the maximum temperature rise limits set by IEC.

Table 7.2 shows the temperature rise at different load currents with unpainted current path, and are the values illustrated in Figure 7.3.

Table 7.2: The temperature rise at different load currents with painted current path

		Temperature rise ΔT [°C]			
Sensor	Placement	630 A	500 A	400 A	200 A
Phase L1					
40	Middle of connection bar	81.0	56.3	37.1	12.1
3	Rotating contact – left	80.5	55.2	37.5	11.4
6	Middle of busbar	69.6	47.3	31.3	10.4
9	Rotating contact – right	67.4	46.4	30.1	10.2
41	Middle of connection bar	59.1	38.7	24.1	8.3
Enclosure surface					
23	Middle of inside, side wall	21.8	14.1	8.9	3.8
26	Middle of inside, top surface	22.4	15.0	9.4	4.0

This is confirmed in Table 7.2, who contains the temperature rise values used in Figure 7.3. The colour green used on the table indicates the temperature measurements on the switches that are within IEC limits. Table 7.2 shows that switches are within IEC temperature rise limit with 500 A, 400 A and 200 A current load.

7.3.3 The temperature rise in L1

Figure 7.4 show the temperature rise with both unpainted and painted conductors for phase L1. The figure for temperature rise in L1 with unpainted and painted showed separately is given in Figure 7.2 and Figure 7.3. The values temperature rise values used in Figure 7.4 is given in Table 7.1 and Table 7.2.

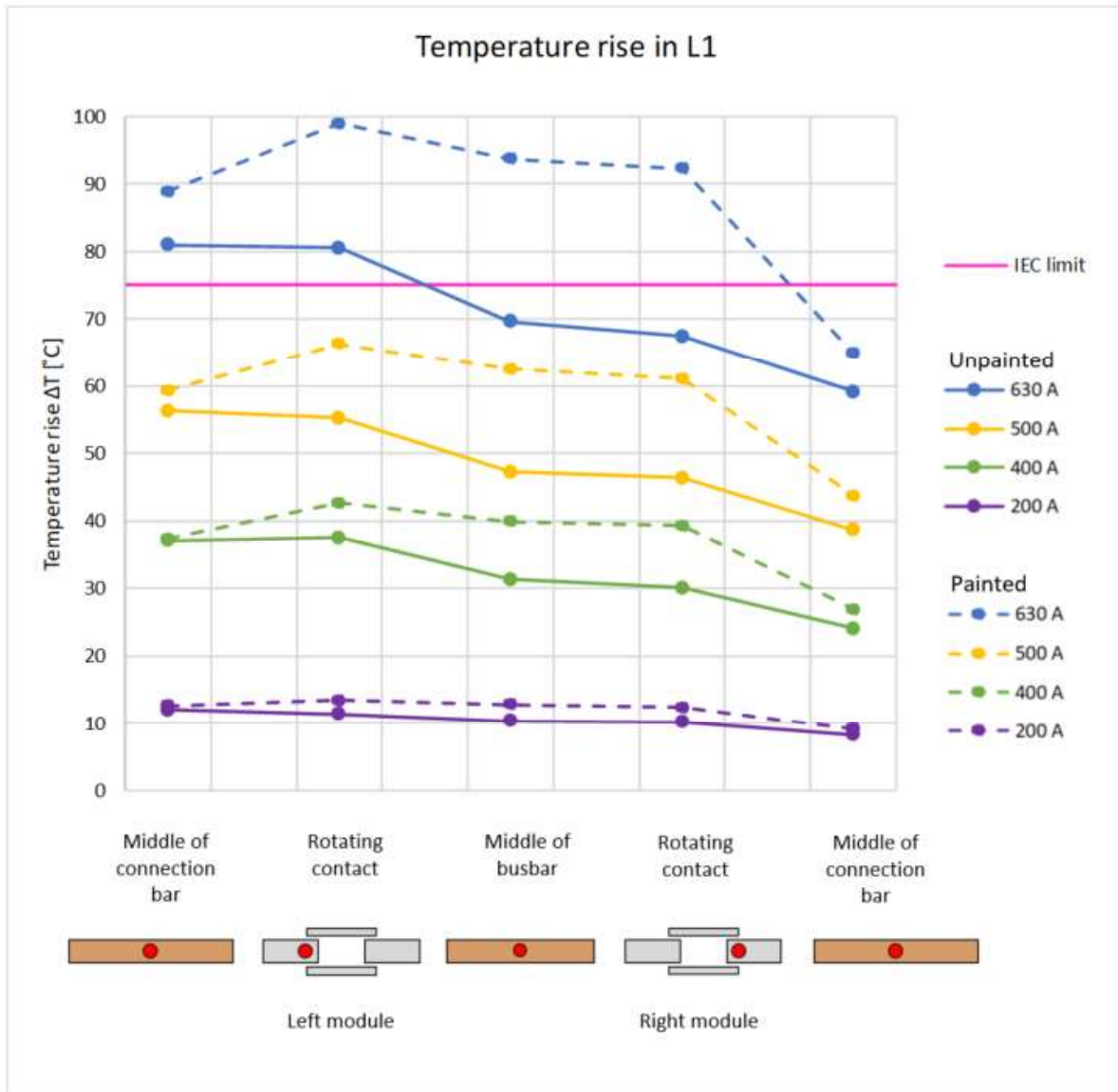


Figure 7.4: Temperature rise in L1

Figure 7.4 shows the temperature rise at different load values for both painted and unpainted conductors. The figure shows that the temperature rise is highest with painted conductors. The temperature difference between painted and unpainted conductors increases with the current load. The largest temperature difference for 630 A is 24.9 °C, the largest difference for 500 A is 15.2 °C, the largest for 400 A is 9.2 °C and 2.5 °C for 200 A. The largest temperature difference is on the middle of the busbar and on the switch on the left module. The smallest difference is on the connection bars on the right module.

The temperature distribution is also different. The largest temperature rise for the unpainted conductors are on the rotating contact on the left module and on the busbar. The largest temperature rise for the unpainted conductors are on the middle of the connection bar and on the rotating contact on the left module.

8 Thermal radiation estimation

This chapter contains the procedure and the estimated thermal radiation.

8.1 Procedure

The thermal radiation for each part of the current path is calculated using equation (2.9). To illustrate which part of the current path who radiates the most and the least amount of thermal radiation, the current path is divided into 5 parts. The connection bar and the switch on the right module, the busbar and the switch/replacement bar and the connection bar on the left module, see Figure 8.1.

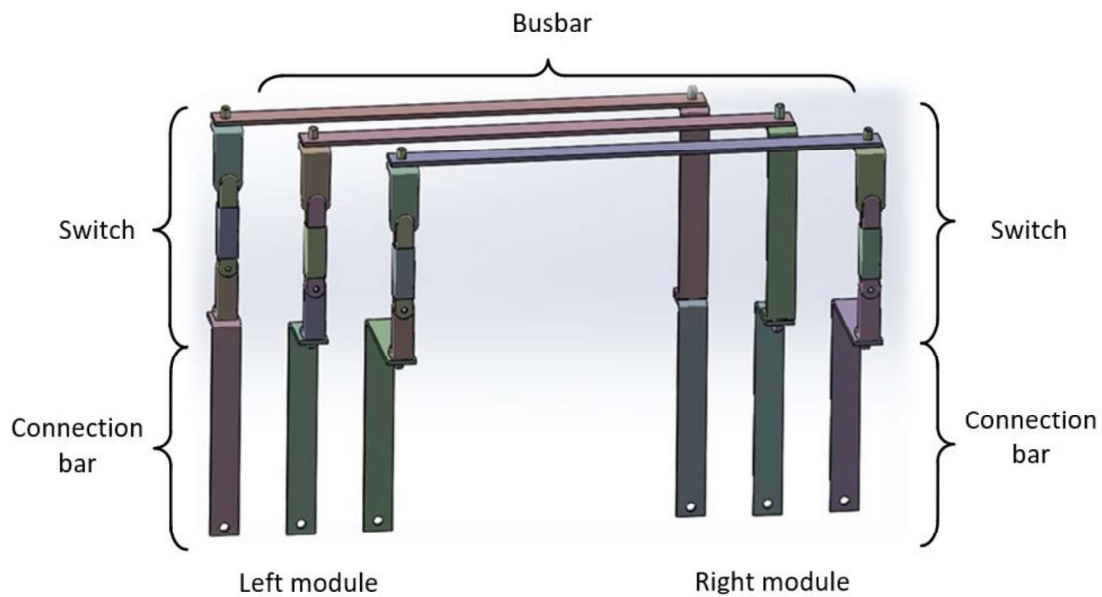


Figure 8.1: Calculation of thermal radiation [15]

The values used for calculating the thermal radiation is found in previous chapters. The emissivity and the view factor are given in Table 8.1. The view factor is chosen to be 0.9.

Table 8.1: Values used when estimating the thermal radiation

	Components	Value
Emissivity	Copper	0.22
	Silver coated copper	0.10
	Paint	0.93
View factor	All	0.9

8.2 Result

The full result and calculation of the thermal radiation estimation for painted and unpainted conductors at different loads are given in appendix G and H.

8.2.1 Thermal radiation with unpainted conductors

The thermal radiation is calculated using equation (2.9), with emissivity and view factor values from Table 8.1, temperature values from appendix F and the surface area from Table 4.1. The thermal radiation on phase L1 with unpainted conductors are given in Table 8.2.

Table 8.2: Thermal radiation on phase L1 with unpainted conductor

		Unpainted [W]			
	Module	630 A	500 A	400 A	200 A
Connection bar	Left	5.6	3.2	1.8	0.5
Switch	Left	1.9	1.1	0.6	0.2
Busbar		8.2	4.6	2.7	0.7
Switch	Right	1.7	1.0	0.6	0.1
Connection bar	Right	3.3	2.0	1.1	0.3

Figure 8.2 shows how much of the total power loss goes to thermal radiation. Using values from Table 8.2 and the total power loss of each component from Table 6.9.

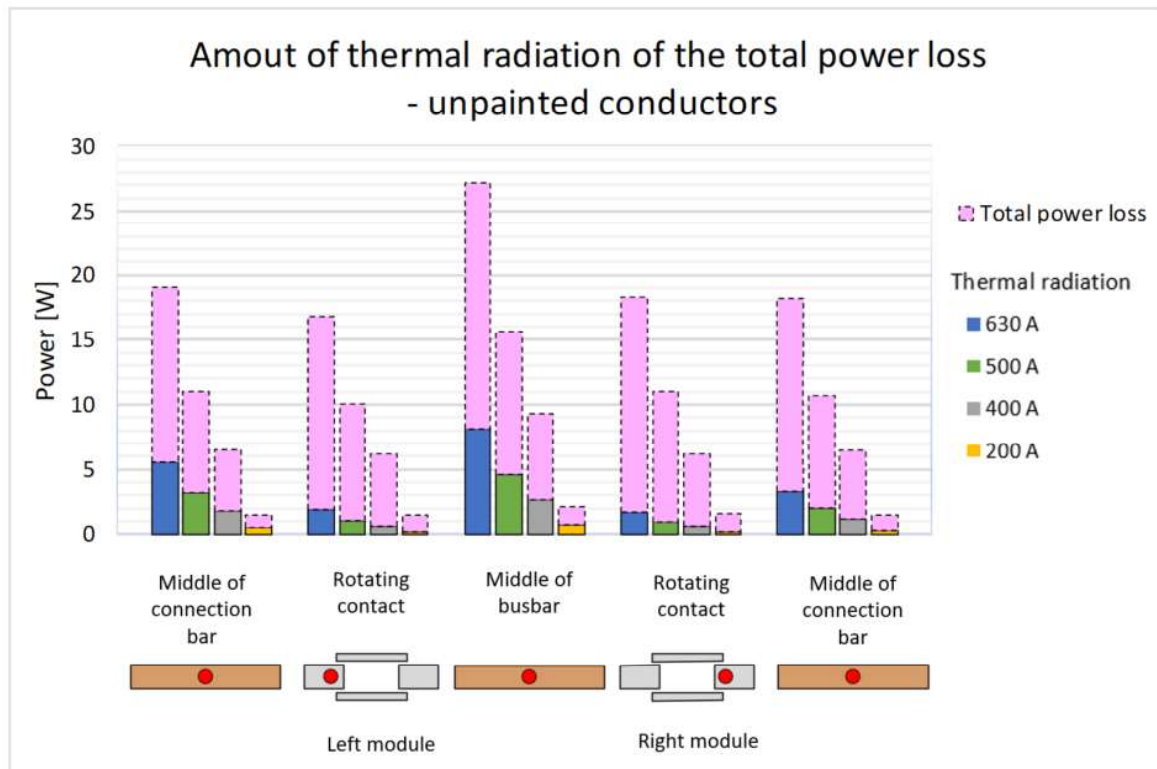


Figure 8.2: Thermal radiation of phase L1 unpainted

8 Thermal radiation estimation

Figure 8.2 shows that the power loss from the switches are approximately 10 % of the total power loss in the switch. The report “Estimating the temperature rise of load break switch contacts in enclosed MV switchgear” reached the same result with an LBS stripped puffer switch. [1] The power loss of the switches can therefore be assumed to be accurate. It is more difficult to determine the accuracy of the connection bars, as the temperature rise at the input might be unnaturally low and making the thermal radiation underestimated. The opposite may happen on the connection bar near the output, which may be overestimated.

Table 8.3 shows how much of the total power loss is thermal radiation in percent. This is calculated using Table 8.2 and the total power loss for each component from Table 6.9.

Table 8.3: The thermal radiation in percent of the total power loss with unpainted conductors

		Unpainted [%]			
	Module	630 A	500 A	400 A	200 A
Connection bar	Left	29	29	28	35
Switch	Left	11	11	10	11
Busbar		30	29	29	34
Switch	Right	9	9	9	9
Connection bar	Right	18	18	18	22

Table 8.3 shows that the percent of thermal radiation is larger for 200 A. This is most likely due to the low temperature rise for a 200 A. As there is no large difference between the initial temperature and the steady state temperature, small deviations may impact the thermal radiation calculations more. Making the 200 A thermal radiation estimate less accurate.

8.2.2 Thermal radiation with painted conductors

The thermal radiation is calculated using equation (2.9), with emissivity and view factor values from Table 8.1, temperature values from appendix F and the surface area from Table 4.1. The thermal radiation on phase L1 with unpainted conductors are given in Table 8.4.

Table 8.4: Thermal radiation on phase L1 with painted conductor

		Painted [W]			
	Module	630 A	500 A	400 A	200 A
Connection bar	Left	19	12	7.2	1.9
Switch	Left	12	7.3	4.6	1.0
Busbar		20	12	7.4	2.3
Switch	Right	9	5.5	3.3	0.9
Connection bar	Right	11	6.4	3.7	1.0

Figure 8.3 shows how much of the total power loss goes to thermal radiation. Using values from Table 8.4 and the total power loss of each component from Table 6.9.

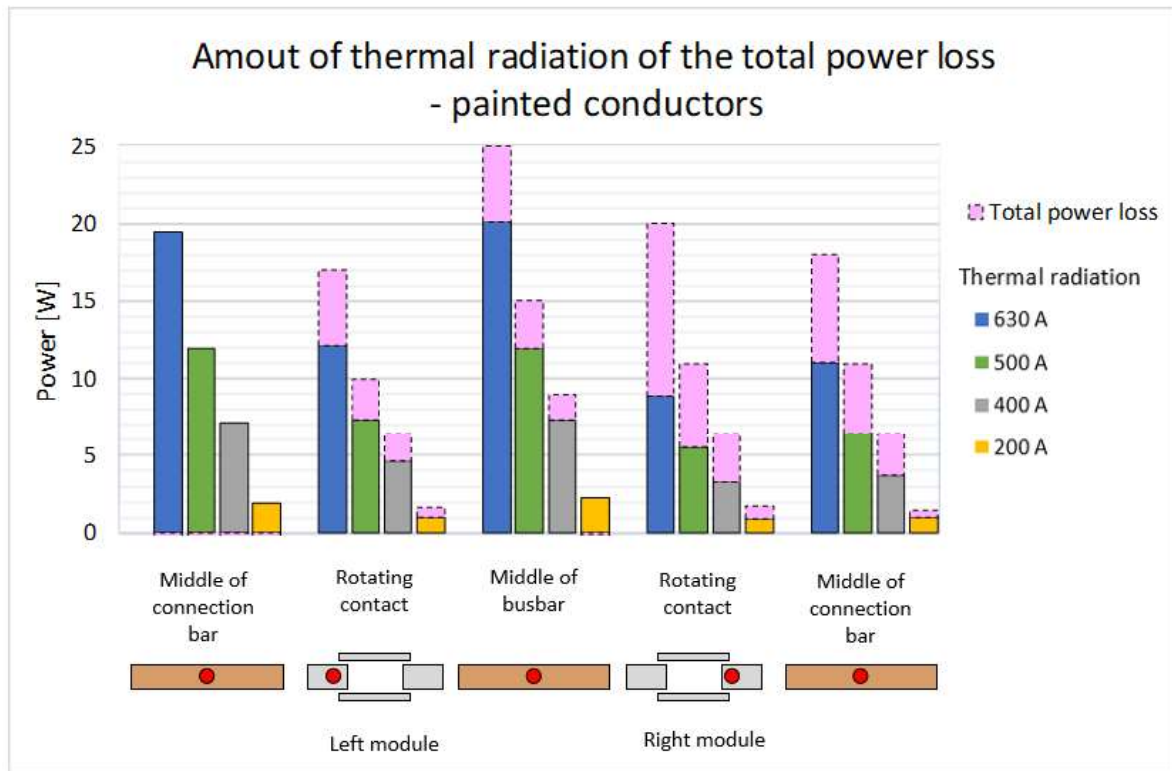


Figure 8.3: Thermal radiation of phase L1 painted

Figure 8.3 shows that the thermal radiation is higher than the total power loss for the connection bar on the left module. This result is most likely severely overestimated. This may also apply the switch in the left module but not necessary to the same extent. The thermal radiation of the connection bar on the right module may be underestimated, because of the temperature loss to the current input.

Figure 8.3 shows that the power loss from the switches are approximately 45-50 % of the total power loss. The report “Estimating the temperature rise of load break switch contacts in enclosed MV switchgear” reached approximately the same result with an LBS stripped puffer switch. [1] The thermal radiation of the switch in the right module is therefore accurate.

Table 8.5 Shows the thermal radiation in percent of the total power loss with painted conductors.

Table 8.5: The thermal radiation in percent of the total power loss with painted conductors

		Painted [%]			
	Module	630 A	500 A	400 A	200 A
Connection bar	Left	103	109	111	125
Switch	Left	72	73	72	65
Busbar		80	80	82	94
Switch	Right	45	50	46	51
Connection bar	Right	62	58	58	66

8 Thermal radiation estimation

Table 8.3 shows that the percent of thermal radiation is largest in the copper bars for 200 A. This is most likely due to the low temperature rise in 200 A, where small variations may affect the result more, making the 200 A thermal radiation estimate less accurate.

9 Discussion

This chapter will contain the discussion the uncertainties in the temperature rise test and the influence of thermal radiation on MV switchgear unit.

9.1 Influence of thermal radiation

The influence of thermal radiation of the total power loss with unpainted and painted conductors in MV switchgear, can be difficult to estimate. Thermal radiation is estimated using equation (2.9) and depends on several parameters. Any inaccuracies, measurement errors, simplifications or deviation between parameters will impact the estimated thermal radiation values and make the final result over- or underestimated. This should be taken into account if the results should be used when simulating the thermal radiation in a MV switchgear unit.

The thermal radiation of the different components with unpainted conductors are close to the expected values, this is especially true for the switches (9-11 %), which matches previous results. [1] The thermal radiation of the connection bar (28-35 %) on the right module are most likely somewhat overestimated because of the high temperature on the current output, while connection bar (18-22 %) on the left module are somewhat underestimated because of the low temperature on the input.

The thermal radiation of the different components of the painted conductor is more difficult to determine and are more over- and underestimated. The estimated thermal radiation of the connection bar (103-125%) and the switch (65-73%) in the left module, are unrealistically high and significantly overestimated. These results should be disregarded. The switch (45-51 %) on the right module, matches previous results. [1]

9.2 Parameters who influences the thermal radiation estimate

The thermal radiation is calculated using equation (2.9) and depends on the flowing parameters MV switchgear unit used for testing, the view factor, the emissivity of the material on the current path, the surface area of the current path, the temperature on the current path, the temperature on the wall of the test devise and the total power loss.

9.2.1 The MV switchgear test devise

The MV switchgear test devise differs substantially from a MV switchgear unit in operation. The measurements done are affected by these differences and it is uncertain how applicable the results found on the test devise are on a MV switchgear unit in operation. Ideally the same test should be done on a MV switchgear in operation at the same environment to evaluate the result of the measurements.

The listed parameters applies for the test devise but can cause substantial uncertainties if the results found by the test devise are applied to a MV switchgear in operation.

- The lack of components who support the current path and mechanisms who opens and closes the switches in the test devise

- Only has four switches
- The switchgear enclosure unit is not sealed tight
- There are no additional cooling mechanism
- No current path and circuit breaker to the transformer
- Don't take initial temperature over or under 20-22 °C into account
- Low temperature rise in the input and high temperature in the output, impacts the heat distribution

9.2.2 The view factor

The view factor is assumed to be 0.9 when estimating the thermal radiation. The value 1 is given to object where one of the objects encapsulates the other. This is valid as the enclosure of the switchgear encapsulates the current path.

The problem with this assumption is that the current path is not one object. The current path consists of 15 objects bolted together in 3 rows. The lack of objects in the enclosure, for support, and for connection to the transformer can also affect the view factor. As the view factor for all the objects may not be the same. To take this into account the view factor is difficult to find without using advanced simulation tools, who can take the radiation from each object into account. For the sake of simplicity, it is therefore assumed that the view factor is 0.9.

9.2.3 The emissivity

Materials with higher emissivity, like paint (0.93), gives very accurate measurements, as materials with high emissivity radiates a lot of energy to detect for the thermal imager. The emissivity of the painted conductors matches values from other sources. [12]

Material with low emissivity gives less accurate measurements, as materials with low emissivity radiates less energy for the thermal imager to detect and depend more on surface treatment. The emissivity found for copper (0.22) and silver coated copper (0.10) are slightly lower than the results from thesis "Heat transfer mechanisms in MV load break switches" by Stein Øygarden, who estimated the emissivity for silver coated copper (0.17) and for copper (0.27). [19] The emissivity measurements are still within the emissivity range for the respective materials, for instance copper can vary on between 0.02 and 0.65 depending on whether material is polished or oxidized. The emissivity result can therefore be assumed to be within acceptable values

9.2.4 The surface area

The surface area for the current path is found using the 3D model of the switchgear. Any deviation between the 3D model and the current path will impact the accuracy of the surface area of the components. The surface area found by using the 3D model is compared to the surface area found using measurements of the current path. There are very little deviation between the two methods. It can be concluded that there are very little inaccuracies in the surface area.

9.2.5 The temperature rise test

The temperature rise test gives accurate temperature measurements taken on the current path and on the enclosure in the MV switchgear test device. These measurements may differ from a MV switchgear unit in operation.

What's most likely affected is the heat distribution. In the test device the temperature at the current input is lower than the rest of the current path, this is most likely due to heat escaping out the current input. The opposite happens on the current output, where the heat gathers, as the current output is short circuited.

9.2.6 Total power loss

Total power loss is calculated using (2.1). The power loss calculated using the measured warm resistance on phase L1 matches the power loss calculated using the estimation and measurements on the components in L1. It can be concluded that the estimated values for the resistance of the components in the current path is accurate.

The total power loss estimate however differs substantially from the power loss estimate done on the same test unit in the master thesis "Power loss measurements in MV switchgear for Cigré-working group. [15] The power loss is larger in the master thesis, as it also included the connections on the current input and output of the current path. This report only includes the current path physically inside the enclosure, and not the current input on the bolts and washers. This makes the power loss in this report smaller than previous results. This may affect the accuracy of the result.

10 Conclusion

The influence of thermal radiation and the temperature rise in MV switchgear depends on whether the conductors are unpainted or painted.

With unpainted conductors the silver coated copper switch thermal radiation contributes with approximately 10 % of the total power loss in the switch. The thermal radiation in the copper bars are higher, than on the switch as they have a higher emissivity. The temperature rise is higher with unpainted conductors and the thermal radiation is lower. When simulating the temperature rise it is important, but not critical, to take the thermal radiation into account, if the conductors are unpainted.

With painted conductors the switch thermal radiation contributes with 45-50 % of the total power loss in the switch. Painting, coating or using other methods to increase the emissivity of the conductors can be used to get a lower temperature rise, but it will give a higher thermal radiation. If the emissivity of the current path is high it is very important to take the thermal radiation into account when simulating temperature rise in MV switchgear as it is such a large part of the total power loss.

Referanser

- [1] Elin Fjeld, Wilhelm Rondeel, Svein Thore Hagen, Magne Saxegaard, «Estimating the temperature rise of load break switch contact in enclosed MV switchgear,» *Cired*, vol. 2017, nr. 1, pp. 136-139.
- [2] ABB, Distribution Automation Handbook, Vaasa, Finland: ABB, 2013.
- [3] Wilhelm Rondeel, EP2416 "Physics in Electrical Engineering", Lecture: "Heat generation", University of South-Eastern Norway, 2018.
- [4] Elin Fjeld, Wilhelm Rondeel, Knut Vaagsaether, Magne Saxegaard, Pål Skryten, Elham Attar, «Thermal design of future medium voltage switchgear,» *Cired*, p. 5, 15.-18. June 2015.
- [5] Wilhelm Rondeel, EP2416 "Physics in Electrical Engineering", Lecture: "Electrical contacts", University of Southeast-Norway, 2018.
- [6] Wilhelm Rondeel, EP2416 "Physics in Electrical Engineering", Lecture: "Energy balance and heat transfer", University of Southeast-Norway, 2018.
- [7] ABB, Switchgear Manual, Cornelsen Verlag, Berlin, 2000.
- [8] NEK, High-voltage switchgear and controlgear : Part 1 : Common specifications, 2017.
- [9] Peter von Böckh and Thomas Wetzel, Heat transfer Basics and Practice, Berlin: Springer-Verlag Berlin Heidelberg, 2012.
- [10] Øyvind Grøn, «Store norske leksikon,» 2018 Feb 20.. [Internett]. Available: <https://snl.no/emissivitet>. [Funnet 23. Jan 2019].
- [11] Fluke Corporation, «TiS Thermal Imaging Scanner User Manual,» 2010. [Internett]. Available: <https://www.instrumart.com/assets/Fluke-TiS-Imager-Manual.pdf>. [Funnet 28. Mars 2019].
- [12] Fluke Corporation, *Ti20 Thermal imager user manual*, 2006 .
- [13] al, Musilová V. et, «11th Cryogenics Conference of the IIR,» Bratislava, 26 - 29 April 2010..
- [14] Yunus A. Cengel, Heat transfer; A practical approach, Reno, Nevada: Mcgraw-Hill, 2002.
- [15] Helland, Sandra, «Power loss measurements in MV switchgear for Cigré-working group,» University of South-Eastern Norway, 2018.
- [16] Biltema, "Varmebestandig lakk,» [Online]. Available: <https://www.biltema.no/bilpleie/bilvedlikehold/vedlikeholdsprodukter/varmebestandig-lakk-2000023755>. [Accessed 29. 04. 2019].

- [17] Optotherm, Inc, «Optotherm thermal imaging,» 2018. [Internett]. Available: <https://www.optotherm.com/emiss-calculating.htm>. [Funnet 2019 04.].
- [18] B. Fluke, «Amazon,» 2019. [Internett]. Available: <https://www.amazon.com/Fluke-Ti25-9Hz-Thermal-Imager/dp/B002I50R6M>. [Funnet 04. 29. 2019].
- [19] Stein Øygarden, «Heat transfer mechanisms in MV load break switches,» University College og Southeast Norway, Porsgrunn, 2017.

Appendices

Appendix A: Task description

Appendix B: The placement of the thermocouple elements

Appendix D: Surface area of the current path

Appendix C: Emissivity results

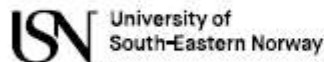
Appendix E: Temperature rise with unpainted and painted current path

Appendix F: Temperature measurements with unpainted and painted conductors

Appendix G: Radiation calculations – Unpainted

Appendix H: Radiation calculations – Painted

Appendix A: Task description



Faculty of Technology, Natural Sciences and Maritime Sciences, Campus Porsgrunn

FMH606 Master's Thesis

Title: Influence of radiation on the temperature rise of MV switchgear

USN supervisor: Elin Fjeld (and Wilhelm Rondeel)

External partner: ABB

Task background:

Cigré (International Council on Large Electric Systems) is an association where experts from all around the world work together in working groups to improve electric power systems. Simulation technologies have an increasing role in the development and verifying the performance of high voltage equipment, and Cigré working group A3.36 is studying to what degree simulations can be used to predict the steady state temperature rise of MV and HV switchgear. When simulating the heat transfer, one challenge is to estimate the influence of radiation.

Task description:

The student should perform temperature rise tests on MV switchgear device(s) and study the influence of radiation. This would involve

- Measurements of the emissivity of the current conductors and enclosure surfaces.
- Change the emissivity (e.g. by painting the parts) and investigate how that influences the result.
- The amount of heat dissipated by radiation is strongly dependent on the absolute temperature. Perform experiments at different temperature ranges (e.g. with different load currents or different enclosures).

In addition (based on the measurements), theoretical considerations should be made to estimate the contribution of heat transfer by radiation.

Student category: EPE

Practical arrangements:

Experimental investigations will take place at USN. A high current injector, infrared camera, and different test objects are available in the lab.

Supervision:

As a general rule, the student is entitled to 15-20 hours of supervision. This includes necessary time for the supervisor to prepare for supervision meetings (reading material to be discussed, etc).

Signatures:

Supervisor (date and signature):

Student (write clearly in all capitalized letters):

Student (date and signature):

Address: Kjølnes ring 56, NO-3918 Porsgrunn, Norway. **Phone:** 35 57 50 00. **Fax:** 35 55 75 47.

Appendix B: The placement of the thermocouple elements


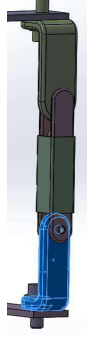
Sensor	Placement, connection type	Module
Phase L1		
1	Brushing connection, bolted Cu-Cu	Left
40	Middle of connection bar	Left
2	Lower switch connection, bolted Cu-Ag	Left
3	Rotating contact	Left
4	Open/close contact	Left
5	Upper switch connection, bolted Cu-Ag	Left
6	Middle of busbar	
7	Upper switch connection, bolted Cu-Ag	Right
8	Open/close contact	Right
9	Rotating contact	Right
10	Lower switch connection, bolted Cu-Ag	Right
41	Middle of connection bar	Right
11	Brushing connection, bolted Cu-Cu	Right
Phase L2		
12	Brushing connection, bolted Cu-Cu	Left
42	Middle of connection bar	Left
13	Lower switch connection, bolted Cu-Ag	Left
14	Rotating contact	Left
15	Open/close contact	Left
16	Upper switch connection, bolted Cu-Ag	Left
17	Middle of busbar	
43	Middle of replacement bar	Right
44	Middle of connection bar	Right
29	Brushing connection, bolted Cu-Cu	Right
Phase L3		
31	Brushing connection, bolted Cu-Cu	Left
45	Middle of connection bar	Left
18	Rotating contact	Left
19	Open/close contact	Left
32	Middle of busbar	
46	Middle of replacement bar	Right
47	Middle of connection bar	Right
30	Brushing connection, bolted Cu-Cu	Right




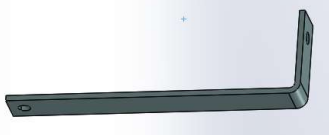

Sensor	Module
In air or on enclosure surface	
20	Inside air, near top of the enclosure
21	Inside air, middle of the enclosure
22	Inside air, near bottom of the enclosure
23	Middle of inside, side wall
24	Middle of inside, back wall
25	Middle of inside, front wall
26	Middle of inside, top surface
27	Middle of outside, side wall
28	Middle of outside, front wall

Appendix C: Surface area of the current path

First method:

Finding the surface area of the current path using a 3D model.

The Switch			
The knife	Area [mm ²]	Overlap [mm ²]	
Front and back	3404		
Sidex2	1628		
Top and bottom	241		
Total	6901.2		
Front and back contact	Area [mm ²]	Overlap [mm ²]	
Frontx2	5860	3404	
Sidex4	2976	1687	
Arc (top/bottom) x4	928		
Total	4673		
Upper connection	Area [mm ²]	Overlap [mm ²]	
Front	3358	1138	
Back	3840	490	
Sides	3894		
Total	9464		
Lower connection	Area [mm ²]	Overlap [mm ²]	
Front	2271	148	
Back	2361	639	
Sides	3988		
Total	7833		
Total	28870 mm ² 0.028870 m ²		

The copper bars			
Replacement bar	Area [mm ²]	Overlap [mm ²]	
Front	11828	3200	
Back	21426	982	
Sides	4628		
Total	33700 0.033700	mm ² m ²	
Busbar	Area [mm ²]	Overlap [mm ²]	
Top and bottom	54190	3200	
Sides and ends	8688		
End	480		
Total	59678 0.059678	mm ² m ²	
Connection bar L1	Area [mm ²]	Overlap [mm ²]	
Front	19368	236	
Back	19745	1712.7	
Sides/ends	6426		
Total	43590 0.043590	mm ² m ²	
Connection bar L2	Area [mm ²]	Overlap [mm ²]	
Front	15448	236	
Back	15825	1712.7	
Sides/ends	5250		
Total	34574 0.034574	mm ² m ²	
Connection bar L3	Area [mm ²]	Overlap [mm ²]	
Front	13857	236	
Back	13480	1712.7	
Sides	4660		
Total	30048 0.030048	mm ² m ²	

Second method:

Finding the surface area by calculating the surface are based upon given measurements.

The surface area of the copper bars is calculated using the following equation:

$$Area = 2 * lenght (Width + depth) - Overlap$$

Areal of the copper bars				
	Replacement bars	Busbar		
Length	330	650	mm	
Width	40	40	mm	
Depth	6	6	mm	
Overlap	0.0034	0.0032	m ²	
Areal	0.03036	0.0598	m ²	
Connection bars				
	L1	L2	L3	
Length	470	370	330	mm
Width	40	40	40	mm
Depth	6	6	6	mm
Overlap	0.0016	0.0016	0.0016	m ²
Areal	0.04324	0.03404	0.03036	m ²

Total areal of the switches						
	Upper switch connection	Upper connection	Front/Back knife	Lower connections	Lower switch connections	
Length	30	80	120	100	30	mm
Width	27	27	25	37	37	mm
Depth	9	9	4	7	7	mm
Overlap	0.00081	-	-	-	0.00	m ²
Areal	0.00135	0.00576	0.00696	0.0088	0.00264	m ²
					Total areal	0.02632 m ²

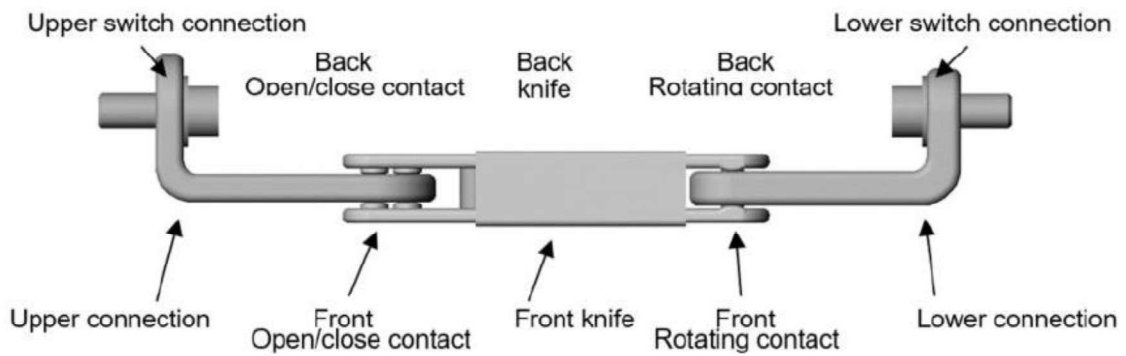


Figure 10.1: The switch [15]

The surface area for all the components using the second method.

Table 10.1: Surface area using the measurements

Surface area [m ²]					
	Connection bar	Switch	Busbar	Switch/replacement bar	Connection bar
L1	0.0416	0.0263	0.0566	0.0263	0.0416
L2	0.0324	0.0263	0.0566	0.0304	0.0324
L3	0.0288	0.0263	0.0566	0.0304	0.0288

Appendix D: Emissivity results

Table 10.2: Emissivity for copper components

	Temp [°C]	Meas. 1	Meas. 2	Meas. 3
Connection bar Left L1	77	0.22	0.25	0.24
Connection bar Left L2	81	0.23	0.22	0.22
Connection bar Left L3	79.2	0.23	0.22	0.24
Replacement bar Right L2	66.4	0.20	0.24	0.20
Connection bar right L2	59.6	0.20	0.19	0.20
			Avr.	0.22

Table 10.3: Emissivity for the switches (silver coated copper)

	Temp [°C]	Meas. 1	Meas. 2	Meas. 3
Switch Left L1	85.6	0.09	0.08	0.10
Switch Left L2	89.22	0.09	0.07	0.08
Switch Left L3	83.2	0.11	0.12	0.13
Switch Right L1	85.45	0.11	0.10	0.12
			Avr.	0.10

Table 10.4: Emissivity measurements of different types of tape

Tape type	Placement	Temp [°C]	Meas. 1	Meas. 2	Meas. 3
El. Tape	Bar left L1	79.4	0.95	0.95	0.95
Masking tape (Tesa)	Bar right L1	61,5	0.98	0.94	0.96
Masking tape (Biltema)	Bar left L2	84.5	0.95	0.96	0.96

Table 10.5: Emissivity measurements of the copper bars using tape

Tape type	Placement	Temp [°C]	Meas. 1	Meas. 2	Meas. 3
El. Tape	Bar left L1	79.4	0.19	0.26	0.20
Masking tape (Tesa)	Bar right L1	61,5	0.22	0.20	0.24
Masking tape (Biltema)	Bar left L2	84.5	0.21	0.19	0.20

Table 10.6: Emissivity painted copper conductors

Placement	Emissivity measurements					
Painted copper Conductors	0.90	0.96	0.95	0.97	0.90	0.91
	0.96	0.90	0.90	0.93	0.94	0.93

Appendix E: Temperature rise with unpainted and painted current path

		Temperature rise ΔT [°C] - unpainted			
Sensor	Placement	630 A	500 A	400 A	200 A
Phase L1					
40	Middle of connection bar	88.8	59.3	37.4	12.7
3	Rotating contact – left	98.9	66.3	42.7	13.5
6	Middle of busbar	93.7	62.5	39.9	12.9
9	Rotating contact – right	92.3	61.1	39.3	12.4
41	Middle of connection bar	64.9	43.7	26.9	9.1
Phase L2					
42	Middle of connection bar	97.8	63.5	40.1	13.1
14	Rotating contact – left	85.8	59.5	37.1	12.7
17	Middle of busbar	90.9	61.9	38.7	12.7
43	Middle of replacement bar	79.7	53.7	33.4	11
44	Middle of connection bar	63.3	43	26.5	8.8
Phase L3					
45	Middle of connection bar	90.7	59.6	39.1	12.9
18	Rotating contact – left	92.8	63.4	40.3	13.4
32	Middle of busbar	90.4	59.8	37.2	12.1
46	Middle of replacement bar	77.1	52.7	33.3	11.3
47	Middle of connection bar	65.9	44.3	32.7	9.4
In air or on enclosure surface					
23	Middle of inside, side wall	18.9	12.6	6.9	2.7
26	Middle of inside, top surface	20.5	14	7.9	3.2

		Temperature rise ΔT [°C] - painted			
Sensor	Placement	630 A	500 A	400 A	200 A
Phase L1					
40	Middle of connection bar	81.0	56.3	37.1	12.1
3	Rotating contact – left	80.5	55.2	37.5	11.4
6	Middle of busbar	69.6	47.3	31.3	10.4
9	Rotating contact - right	67.4	46.4	30.1	10.2
41	Middle of connection bar	59.1	38.7	24.1	8.3
Phase L2					
42	Middle of connection bar	93.4	65.3	42.1	13.5
14	Rotating contact - left	78.6	54.0	35.3	12.0
17	Middle of busbar	67.8	45.6	29.2	10.0
43	Middle of replacement bar	62.7	41.8	26.7	9.1
44	Middle of connection bar	54.7	36.0	22.8	7.8
Phase L3					
45	Middle of connection bar	84.6	58.6	38.1	12.5
18	Rotating contact - left	75.2	51.9	33.8	11.2
32	Middle of busbar	64.7	43.0	27.6	9.4
46	Middle of replacement bar	62.0	46.1	26.3	8.9
47	Middle of connection bar	55.3	36.2	23.1	7.8
In air or on enclosure surface					
23	Middle of inside, side wall	21.8	14.1	8.9	3.8
26	Middle of inside, top surface	22.4	15.0	9.4	4.0

Appendix F: Temperature measurements with unpainted and painted conductors

Steady state temperature with 630 A load			Time to steady state: ca. 5 hours, $T_0 = 21.2\text{ }^\circ\text{C}$			
			Ts [°C]	ΔT [°C]	Ts [°C]	ΔT [°C]
Sensor		Module	Unpainted		Painted	
Phase L1			Unpainted		Painted	
1	Brushing connection, bolted Cu-Cu	Left	106.0	84.8	109.2	88
40	Middle of connection bar	Left	110.0	88.8	102.2	81
2	Lower switch connection, bolted Cu-Ag	Left	118.1	96.9	101.4	80.2
3	Rotating contact	Left	120.1	98.9	101.7	80.5
4	Open/close contact	Left	120.3	99.1	97.2	76
5	Upper switch connection, bolted Cu-Ag	Left	119.6	98.4	96.9	75.7
6	Middle of busbar		114.9	93.7	90.8	69.6
7	Upper switch connection, bolted Cu-Ag	Right	116.3	95.1	92.0	70.8
8	Open/close contact	Right	116.0	94.8	91.5	70.3
9	Rotating contact	Right	113.5	92.3	88.6	67.4
10	Lower switch connection, bolted Cu-Ag	Right	106.5	85.3	89.5	68.3
41	Middle of connection bar	Right	86.1	64.9	80.3	59.1
11	Brushing connection, bolted Cu-Cu	Right	72.2	51	75	53.8
Phase L2			Unpainted		Painted	
12	Brushing connection, bolted Cu-Cu	Left	121.0	99.8	134	112.8
42	Middle of connection bar	Left	119.0	97.8	114.6	93.4
13	Lower switch connection, bolted Cu-Ag	Left	119.0	97.8	104.2	83
14	Rotating contact	Left	107.0	85.8	99.8	78.6
15	Open/close contact	Left	115.9	94.7	85.8	64.6
16	Upper switch connection, bolted Cu-Ag	Left	115.6	94.4	94.2	73
17	Middle of Busbar		112.1	90.9	89.0	67.8
43	Middle of replacement bar	Right	100.9	79.7	83.9	62.7
44	Middle of connection bar	Right	84.5	63.3	75.9	54.7
29	Brushing connection, bolted Cu-Cu	Right	73.1	51.9		
Phase L3			Unpainted			
31	Brushing connection, bolted Cu-Cu	Left	110.6	89.4	119.6	98.4
45	Middle of connection bar	Left	111.9	90.7	105.8	84.6

18	Rotating contact	Left	114.0	92.8	96.4	75.2
19	Open/close contact	Left	114.0	92.8		
32	Middle of busbar		111.6	90.4	85.9	64.7
46	Middle of replacement bar	Right	98.3	77.1	83.2	62.0
47	Middle of connection bar	Right	87.1	65.9	76.5	55.3
30	Brushing connection, bolted Cu-Cu	Right	72.5	51.3	60.6	39.4

Steady state temperature with 630 A load		Time to steady state: ca. 5 hours, $T_0 = 21.2^\circ\text{C}$			
		T_s [°C]	ΔT [°C]	T_s [°C]	ΔT [°C]
Sensor	Module				
In air or on enclosure surface		Unpainted		Painted	
20	Inside air, near top of the enclosure	59.8	38.6		
21	Inside air, middle of the enclosure	48.3	27.1		
22	Inside air, near bottom of the enclosure	36.4	15.2		
23	Middle of inside, side wall	40.1	18.9	43.0	21.8
24	Middle of inside, back wall	43.7	22.5		
25	Middle of inside, front wall	36.4	15.2		
26	Middle of inside, top surface	41.7	20.5	43.6	22.4
27	Middle of outside, side wall	33.2	12		
28	Middle of outside, front wall	37.9	16.7		

Steady state temperature with 500 A load			Time to steady state: ca. 5 hours, $T_0 = 21.1\text{ °C}$			
			Ts [°C]	ΔT [°C]	Ts [°C]	ΔT [°C]
Sensor		Module	Unpainted		Painted	
Phase L1			Unpainted		Painted	
1	Brushing connection, bolted Cu-Cu	Left	78.5	57.4	82.5	61.4
40	Middle of connection bar	Left	80.4	59.3	77.4	56.3
2	Lower switch connection, bolted Cu-Ag	Left	86.5	65.4	76.3	55.2
3	Rotating contact	Left	87.4	66.3	76.3	55.2
4	Open/close contact	Left	87.1	66.0	73.0	51.9
5	Upper switch connection, bolted Cu-Ag	Left	87.2	66.1	72.8	51.7
6	Middle of busbar		83.6	62.5	68.4	47.3
7	Upper switch connection, bolted Cu-Ag	Right	84.2	63.1	69.3	48.2
8	Open/close contact	Right	84.0	62.9	68.9	47.8
9	Rotating contact	Right	82.2	61.1	67.5	46.4
10	Lower switch connection, bolted Cu-Ag	Right	77.9	56.8	67.3	46.2
41	Middle of connection bar	Right	64.8	43.7	59.8	38.7
11	Brushing connection, bolted Cu-Cu	Right	56.3	35.2	55.0	33.9
Phase L2			Unpainted		Painted	
12	Brushing connection, bolted Cu-Cu	Left	88.6	67.5	-	-
42	Middle of connection bar	Left	84.6	63.5	86.4	65.3
13	Lower switch connection, bolted Cu-Ag	Left	88.1	67	78.5	57.4
14	Rotating contact	Left	80.6	59.5	75.1	54
15	Open/close contact	Left	86.3	65.2	65.3	44.2
16	Upper switch connection, bolted Cu-Ag	Left	86.1	65	71.0	49.9
17	Middle of Busbar		83.0	61.9	66.7	45.6
43	Middle of replacement bar	Right	74.8	53.7	62.9	41.8
44	Middle of connection bar	Right	64.1	43	57.1	36
29	Brushing connection, bolted Cu-Cu	Right	55.5	34.4	53.0	31.9
Phase L3			Unpainted			
31	Brushing connection, bolted Cu-Cu	Left	81.9	60.8	89.0	67.9
45	Middle of connection bar	Left	80.7	59.6	79.7	58.6
18	Rotating contact	Left	84.5	63.4	73.0	51.9

19	Open/close contact	Left	84.3	63.2		
32	Middle of busbar		80.9	59.8	64.1	43
46	Middle of replacement bar	Right	73.8	52.7	67.2	46.1
47	Middle of connection bar	Right	65.4	44.3	57.3	36.2
30	Brushing connection, bolted Cu-Cu	Right	56.1	35	52.7	31.6

Steady state temperature with 500 A load		Time to steady state: ca. 5 hours, $T_0 = 21.1\text{ °C}$			
		T_s [°C]	ΔT [°C]	T_s [°C]	ΔT [°C]
Sensor	Module	Unpainted		Painted	
In air or on enclosure surface					
20	Inside air, near top of the enclosure	41.2	20.1		
21	Inside air, middle of the enclosure	40.7	19.6		
22	Inside air, near bottom of the enclosure	31.4	10.3		
23	Middle of inside, side wall	33.7	12.6	35.2	14.1
24	Middle of inside, back wall	36.1	15		
25	Middle of inside, front wall	32.3	11.2		
26	Middle of inside, top surface	35.1	14	36.1	15.0
27	Middle of outside, side wall	29.3	8.2		
28	Middle of outside, front wall	32.4	11.3		

Steady state temperature with 400 A load			Time to steady state: ca. 4 hours, $T_0 = 21.9\text{ }^\circ\text{C}$			
			Ts [°C]	ΔT [°C]	Ts [°C]	ΔT [°C]
Sensor		Module	Unpainted		Painted	
Phase L1			Unpainted		Painted	
1	Brushing connection, bolted Cu-Cu	Left	58.0	36.1	62.1	40.2
40	Middle of connection bar	Left	59.3	37.4	59.0	37.1
2	Lower switch connection, bolted Cu-Ag	Left	63.8	41.9	59.0	37.1
3	Rotating contact	Left	64.6	42.7	59.4	37.5
4	Open/close contact	Left	64.7	42.8	56.6	34.7
5	Upper switch connection, bolted Cu-Ag	Left	64.4	42.5	56.4	34.5
6	Middle of busbar		61.8	39.9	53.1	31.2
7	Upper switch connection, bolted Cu-Ag	Right	62.2	40.3	53.3	31.4
8	Open/close contact	Right	62.1	40.2	53.1	31.2
9	Rotating contact	Right	61.2	39.3	52.0	30.1
10	Lower switch connection, bolted Cu-Ag	Right	58.1	36.2	51.6	29.7
41	Middle of connection bar	Right	48.8	26.9	46.2	24.3
11	Brushing connection, bolted Cu-Cu	Right	44.2	22.3	42.8	20.9
Phase L2			Unpainted		Painted	
12	Brushing connection, bolted Cu-Cu	Left	63.7	41.8	72.7	50.8
42	Middle of connection bar	Left	62.0	40.1	64.1	42.2
13	Lower switch connection, bolted Cu-Ag	Left	64.1	42.2	59.4	37.5
14	Rotating contact	Left	59.0	37.1	57.2	35.3
15	Open/close contact	Left	63.0	41.1	50.6	28.7
16	Upper switch connection, bolted Cu-Ag	Left	62.0	40.1	54.4	32.5
17	Middle of Busbar		60.6	38.7	51.1	29.2
43	Middle of replacement bar	Right	55.3	33.4	48.6	26.7
44	Middle of connection bar	Right	48.4	26.5	44.7	22.8
29	Brushing connection, bolted Cu-Cu	Right	43.2	21.3	42.0	20.1
Phase L3			Unpainted		Painted	
31	Brushing connection, bolted Cu-Cu	Left	60.0	38.1	65.7	43.8
45	Middle of connection bar	Left	61.0	39.1	60.0	38.1
18	Rotating contact	Left	62.2	40.3	55.7	33.8

19	Open/close contact	Left	61.8	39.9		
32	Middle of busbar		59.1	37.2	49.5	27.6
46	Middle of replacement bar	Right	55.2	33.3	48.2	26.3
47	Middle of connection bar	Right	54.6	32.7	45.0	23.1
30	Brushing connection, bolted Cu-Cu	Right	43.6	21.7	42.1	20.2

Steady state temperature with 400 A load		Time to steady state: ca. 4 hours, $T_0 = 21.9\text{ }^\circ\text{C}$			
		T_s [°C]	ΔT [°C]	T_s [°C]	ΔT [°C]
Sensor	Module	Unpainted		Painted	
In air or on enclosure surface					
20	Inside air, near top of the enclosure	37.1	15.2		
21	Inside air, middle of the enclosure	33.3	11.4		
22	Inside air, near bottom of the enclosure	27.5	5.6		
23	Middle of inside, side wall	28.8	6.9	30.8	8.9
24	Middle of inside, back wall	30.0	8.1		
25	Middle of inside, front wall	27.8	5.9		
26	Middle of inside, top surface	29.8	7.9	31.3	9.4
27	Middle of outside, side wall	26.1	4.2		
28	Middle of outside, front wall	28.0	6.1		

Steady state temperature with 200 A load			Time to steady state: ca. 4 hours, $T_0 = 20.5\text{ }^\circ\text{C}$			
			Ts [°C]	ΔT [°C]	Ts [°C]	ΔT [°C]
Sensor		Module	Unpainted		Painted	
Phase L1			Unpainted		Painted	
1	Brushing connection, bolted Cu-Cu	Left	32.5	12	32.4	11.9
40	Middle of connection bar	Left	33.2	12.7	32.6	12.1
2	Lower switch connection, bolted Cu-Ag	Left	33.9	13.4	31.9	11.4
3	Rotating contact	Left	34.0	13.5	31.9	11.4
4	Open/close contact	Left	34.1	13.6	31.5	11
5	Upper switch connection, bolted Cu-Ag	Left	34.1	13.6	31.6	11.1
6	Middle of busbar		33.4	12.9	30.9	10.4
7	Upper switch connection, bolted Cu-Ag	Right	33.4	12.9	31.1	10.6
8	Open/close contact	Right	33.2	12.7	31.1	10.6
9	Rotating contact	Right	32.9	12.4	30.7	10.2
10	Lower switch connection, bolted Cu-Ag	Right	32.0	11.5	30.3	9.8
41	Middle of connection bar	Right	29.6	9.1	28.8	8.3
11	Brushing connection, bolted Cu-Cu	Right	27.7	7.2	28.3	7.8
Phase L2			Unpainted		Painted	
12	Brushing connection, bolted Cu-Cu	Left	34.7	14.2	34.7	14.2
42	Middle of connection bar	Left	33.6	13.1	34.0	13.5
13	Lower switch connection, bolted Cu-Ag	Left	34.7	14.2	32.8	12.3
14	Rotating contact	Left	33.2	12.7	32.5	12
15	Open/close contact	Left	34.3	13.8	30.5	10
16	Upper switch connection, bolted Cu-Ag	Left	34.3	13.8	31.7	11.2
17	Middle of Busbar		33.2	12.7	30.5	10
43	Middle of replacement bar	Right	31.5	11	29.6	9.1
44	Middle of connection bar	Right	29.3	8.8	28.3	7.8
29	Brushing connection, bolted Cu-Cu	Right	27.5	7	27.7	7.2
Phase L3			Unpainted		Painted	
31	Brushing connection, bolted Cu-Cu	Left	33.4	12.9	33.7	13.2
45	Middle of connection bar	Left	33.4	12.9	33.0	12.5
18	Rotating contact	Left	33.9	13.4	31.7	11.2

19	Open/close contact	Left	33.6	13.1	31.2	10.7
32	Middle of busbar		32.6	12.1	29.9	9.4
46	Middle of replacement bar	Right	31.8	11.3	29.4	8.9
47	Middle of connection bar	Right	29.9	9.4	28.4	7.9
30	Brushing connection, bolted Cu-Cu	Right	27.6	7.1	27.7	7.2

Steady state temperature with 400 A load		Time to steady state: ca. 4 hours, $T_0 = 20.5\text{ }^\circ\text{C}$			
		T_s [°C]	ΔT [°C]	T_s [°C]	ΔT [°C]
Sensor	Module				
In air or on enclosure surface		Unpainted		Painted	
20	Inside air, near top of the enclosure	24.9	4.4	26.3	5.8
21	Inside air, middle of the enclosure	24.8	4.3	25.7	5.2
22	Inside air, near bottom of the enclosure	22.8	2.3	24.4	3.9
23	Middle of inside, side wall	23.2	2.7	24.3	3.8
24	Middle of inside, back wall	23.5	3	24.6	4.1
25	Middle of inside, front wall	23.0	2.5	24.2	3.7
26	Middle of inside, top surface	23.7	3.2	24.5	4
27	Middle of outside, side wall	22.5	2	23.7	3.2
28	Middle of outside, front wall	23.0	2.5	23.7	3.2

Appendix G: Radiation calculations – Unpainted

	Components	Value
Emissivity	Copper	0.22
	Silver coated copper	0.10
View factor	All	0.90

Emissivity and Surface Area					
Emissivity					
	Connection bar	Switch	Busbar	Switch/replacement bar	Connection bar
L1	0.22	0.10	0.22	0.10	0.22
L2	0.22	0.10	0.22	0.22	0.22
L3	0.22	0.10	0.22	0.22	0.22
Surface area [m ²]					
	Connection bar	Switch	Busbar	Switch/replacement bar	Connection bar
L1	0.0416	0.0263	0.0566	0.0263	0.0416
L2	0.0320	0.0263	0.0566	0.0304	0.0320
L3	0.0288	0.0263	0.0566	0.0304	0.0288

Sensor					
Sensors Ts [°K]					
	Connection bar	Switch	Busbar	Switch/replacement bar	Connection bar
L1	S40	S3	S6	S9	S41
L2	S42	S14	S17	S43	S44
L3	S45	S18	S32	S46	S47
Sensors Tw [°K]					
	Connection bar	Switch	Busbar	Switch/replacement bar	Connection bar
All	S23	S23	S26	S23	S23

Radiation calculations with 630 A					
T _s [°K]					
	Connection bar	Switch	Busbar	Switch/replacement bar	Connection bar
L1	383	393	388	387	359
L2	392	380	385	374	358
L3	385	387	385	364	360
T _w [°K]					
	Connection bar	Switch	Busbar	Switch/replacement bar	Connection bar
L1	313	313	315	313	313
L2	313	313	315	313	313
L3	313	313	315	313	313
P _{rad} [W]					
	Connection bar	Switch	Busbar	Switch/replacement bar	Connection bar
L1	5.6	1.9	8.2	1.7	3.3
L2	5.1	1.5	7.8	3.4	2.5
L3	4.0	1.7	7.7	2.7	2.3
Total	59 W				
P _{rad}	24 % of the total power loss 253 W				

Radiation calculations with 500 A					
T _s [°K]					
	Connection bar	Switch	Busbar	Switch/replacement bar	Connection bar
L1	354	361	357	355	338
L2	358	354	356	349	337
L3	354	358	354	347	339
T _w [°K]					
	Connection bar	Switch	Busbar	Switch/replacement bar	Connection bar
L1	307	307	308	307	307
L2	307	307	308	307	307
L3	307	307	308	307	307
P _{rad} [W]					
	Connection bar	Switch	Busbar	Switch/replacement bar	Connection bar
L1	3.2	1.1	4.6	1.0	2.0
L2	2.7	0.9	4.5	2.0	1.5
L3	2.2	1.0	4.3	1.9	1.4
Total	34 W				
P _{rad}	23 % of the total power loss 151 W				

Radiation calculations with 400 A					
T _s [°K]					
	Connection bar	Switch	Busbar	Switch/replacement bar	Connection bar
L1	332	338	335	334	322
L2	335	332	334	328	322
L3	334	335	332	328	328
T _w [°K]					
	Connection bar	Switch	Busbar	Switch/replacement bar	Connection bar
L1	302	302	303	302	302
L2	302	302	303	302	302
L3	302	302	303	302	302
P _{rad} [W]					
	Connection bar	Switch	Busbar	Switch/replacement bar	Connection bar
L1	1.8	0.6	2.7	0.6	1.1
L2	1.6	0.5	2.5	1.1	0.9
L3	1.3	0.6	2.4	1.1	1.0
Total	20 W				
P _{rad}	21 % of the total power loss 91 W				

Radiation calculations with 200 A					
T _s [°K]					
	Connection bar	Switch	Busbar	Switch/replacement bar	Connection bar
L1	306	307	307	306	303
L2	307	306	306	305	302
L3	307	307	306	305	303
T _w [°K]					
	Connection bar	Switch	Busbar	Switch/replacement bar	Connection bar
L1	296	296	297	296	296
L2	296	296	297	296	296
L3	296	296	297	296	296
P _{rad} [W]					
	Connection bar	Switch	Busbar	Switch/replacement bar	Connection bar
L1	0.53	0.16	0.72	0.14	0.33
L2	0.44	0.15	0.70	0.31	0.25
L3	0.38	0.16	0.65	0.32	0.25
Total	5.5 W				
P _{rad}	26 % of the total power loss 21.5 W				

Appendix H: Radiation calculations – Painted

	Components	Value
Emissivity	Painted conductors	0.93
View factor	All	0.9

Emissivity and Surface Area					
Emissivity					
	Connection bar	Switch	Busbar	Switch/replacement bar	Connection bar
L1	0.93	0.93	0.93	0.93	0.93
L2	0.93	0.93	0.93	0.93	0.93
L3	0.93	0.93	0.93	0.93	0.93
Surface area [m ²]					
	Connection bar	Switch	Busbar	Switch/replacement bar	Connection bar
L1	0.0416	0.0263	0.0566	0.0263	0.0416
L2	0.0320	0.0263	0.0566	0.0304	0.0320
L3	0.0288	0.0263	0.0566	0.0304	0.0288

Sensor					
Sensors Ts [°K]					
	Connection bar	Switch	Busbar	Switch/replacement bar	Connection bar
L1	S40	S3	S6	S9	S41
L2	S42	S14	S17	S43	S44
L3	S45	S18	S32	S46	S47
Sensors Tw [°K]					
	Connection bar	Switch	Busbar	Switch/replacement bar	Connection bar
All	S23	S23	S26	S23	S23

Radiation calculations with 630 A					
T _s [°K]					
	Connection bar	Switch	Busbar	Switch/replacement bar	Connection bar
L1	376	375	364	362	354
L2	388	373	362	357	349
L3	379	370	359	356	350
T _w [°K]					
	Connection bar	Switch	Busbar	Switch/replacement bar	Connection bar
L1	316	316	317	316	316
L2	316	316	317	316	316
L3	316	316	317	316	316
P _{rad} [W]					
	Connection bar	Switch	Busbar	Switch/replacement bar	Connection bar
L1	19.5	12.2	20.1	8.9	11.1
L2	19.4	11.7	19.2	9.0	7.5
L3	14.5	10.8	17.6	8.8	6.8
Total P _{rad}	197 W 76 % of the total power loss 258 W				

Radiation calculations with 500 A					
T _s [°K]					
	Connection bar	Switch	Busbar	Switch/replacement bar	Connection bar
L1	351	350	342	341	333
L2	342	348	340	336	330
L3	353	346.	337	340	330
T _w [°K]					
	Connection bar	Switch	Busbar	Switch/replacement bar	Connection bar
L1	308	308	309	308	308
L2	308	308	309	308	308
L3	308	308	309	308	308
P _{rad} [W]					
	Connection bar	Switch	Busbar	Switch/replacement bar	Connection bar
L1	12.0	7.3	12.0	5.5	6.4
L2	7.0	7.0	11.3	5.4	4.4
L3	8.8	6.6	10.2	6.3	3.9
Total P _{rad}	114 W 76 % of the total power loss 151 W				

Radiation calculations with 400 A					
T _s [°K]					
	Connection bar	Switch	Busbar	Switch/replacement bar	Connection bar
L1	332	333	326	325	319
L2	337	330	324	322	318
L3	333	3289	323	321	318
T _w [°K]					
	Connection bar	Switch	Busbar	Switch/replacement bar	Connection bar
L1	304	304	305	304	304
L2	304	304	305	304	304
L3	304	304	305	304	304
P _{rad} [W]					
	Connection bar	Switch	Busbar	Switch/replacement bar	Connection bar
L1	7.2	4.6	7.4	3.3	3.7
L2	6.8	4.2	6.6	3.1	2.6
L3	5.2	4.0	6.0	3.1	2.3
Total P _{rad}	70 W 76 % of the total power loss 93 W				

Radiation calculations with 200 A					
T _s [°K]					
	Connection bar	Switch	Busbar	Switch/replacement bar	Connection bar
L1	306	305	305	304	302
L2	307	306	306	303	302
L3	306	305	305	303	302
T _w [°K]					
	Connection bar	Switch	Busbar	Switch/replacement bar	Connection bar
L1	298	298	298	298	298
L2	298	298	298	298	298
L3	298	298	298	298	298
P _{rad} [W]					
	Connection bar	Switch	Busbar	Switch/replacement bar	Connection bar
L1	1.9	1.0	2.3	0.9	1.0
L2	1.7	1.1	2.5	0.8	0.7
L3	1.4	1.0	2.2	0.8	0.6
Total P _{rad}	20 W 92 % of the total power loss 21.6 W				